Optimized Simultaneous Surface-Atmosphere Retrieval from Copernicus Sentinel-3 (OSSAR-CS3) - Algorithm Theoretical Basis Document (ATBD)

Doc.No. : EUM/SEN3/DOC/21/1243792
Issue : v1
Date : 3 September 2021
WBS/DBS :

EUMETSAT
Eumetsat-Allee 1, D-64295 Darmstadt, Germany
Tel: +49 6151 807-7
Fax: +49 6151 807 555
http://www.eumetsat.int

© EUMETSAT
The copyright of this document is the property of EUMETSAT.

Page left intentionally blank

Change Record

Version	Date	DCR* No. *if applicable*	Description of Changes
1.0	14/10/2021		Initial Version

DCR = Document Change Request

Table of Contents

Table of Tables

1 INTRODUCTION

1.1 Scope

This is the reference Algorithm Theoretical Basis Document (ATBD) supporting the processor dedicated to the Optimized Simultaneous Surface-Aerosol Retrieval for Copernicus Sentinel-3 (OSSAR-CS3) in Near-Real Time (NRT – strictly less than 3h since the sensing time). The NRT aerosol retrieval is primarily based on the Sea & Land Surface Temperature Radiometer (SLSTR), from both Copernicus S3A & S3B satellites, operationally produced with no interruption from the EUMETSAT S3 Ground-Segment (GS), located in Darmstadt, Germany. Its performance, validation and evolution are completely monitored under the leadership of the EUMETSAT S3 team involving Level 1 (L1) & Level 2 (L2) scientists, system engineer performance, and mission operator teams 24/24h, 7/7 days, in a timely manner compatible with the NRT requirement.

This processor, as well as any related documents, are directly procured under the sole EUMETSAT responsibility, endorsed by the European Commission (EC) / Copernicus mandate. This ATBD includes significant scientific contributions from:

- The original aerosol dual-view prototype from the Swansea University (SU) & its associated ATBD.
- Ideas and developments prototyped & implemented by the EUMETSAT Cloud & Aerosol (CLA) team within the Remote Sensing Products (RSP) division.
- Additional analyses & synthetic data procured by the Finnish Meteorological Institute (FMI) within the framework of the SLSTR Aerosol Retrieval Performance (SARP) project, procured and funded by the EUMETSAT Member States https://www.eumetsat.int/SARP.

The strategy of the OSSAR-CS3 algorithm prototyping, processor development, Calibration & Validation (CalVal), and quality monitoring is overall in line with the EUMETSAT strategy implemented in its Scientific Roadmap for the development of operational aerosol products [RD-1]. In particular, it focuses on optimizing the Simultaneous Surface-Aerosol Retrieval (SSAR) concept for SLSTR. **A key goal of such an optimization is to establish a high degree of resiliency to any past & future changes in the dual-view direction for ensuring a consistently high quality over all geographical areas (*i.e.* global.).**

Technically, this processor reuses several elements of a precursor processor v1, designed and developed by the Copernicus S3 Mission Performance Centre (S3MPC), procured by the European Space Agency (ESA). This precursor v1 was then in-depth revised & optimized by EUMETSAT to increase its scientific maturity for an operational purpose.

The scientific maturity & quality label associated with the OSSAR-CS3, since the deployment of the baseline Collection (BC) 2 in October 2021 is overall Preliminary operational for all surfaces (ocean and lands).

The overall rational of the Collection 2 release is explained in [RD-6]. Its scientific quality is considered to be approaching the expected requirements, and it is considered to have reached a level of maturity which can be safely exploited by users. To ramp up toward its higher maturity level, validation is being performed over longer time series with a larger set of ground-

based measurements, with deeper analysis and fine-tuning continuing until full 'operational' maturity is reached, *i.e.* matching the expected quality requirements, within the year.

1.2 Applicable Documents

	Document Title	Reference
AD-1	Sentinel-3 Product Notice (PN) – SLSTR Level 2 (L2) near Real Time (NRT) Aerosols	EUM/SEN3/DOC/20/1188082 V3.0 Written by J. Chimot (EUMETSAT), October 2021.
AD-2	EUMETSAT Sentinel-3 NRT Atmospheric Composition webpage:	https://www.eumetsat.int/website/home/Satellites/CurrentSatellites/Sentinel3/AtmosphericComposition/index.html
AD-3	Sentinel-3 Mission Requirements Traceability Document (MRTD), C. Donlon, EOP-SM/2184/CDcd, 2011:	https://sentinel.esa.int/documents/247904/1848151/Sentinel-3-Mission-Requirements-Traceability
AD-4	EUMETSAT – Copernicus Sentinel-3 SLSTR L2 NRT AOD Product Data Format (PDF) Specification	EUM/SEN3/DOC/20/1180730 v1.B, written by J. Chimot, October 2021: https://www.eumetsat.int/media/47197
AD-5	Information and documentation about the SLSTR L1B product can be found at:	https://www.eumetsat.int/sea-surface-temperature-services

1.3 Reference Documents

	Document Title	Reference
RD-1	Scientific Scientific Roadmap for the Development of Aerosol Products	EUM/TSS/PLN/17/910992
RD-2	EUMETSAT – Atmospheric Aerosol Optical Depth retrieval performance from Sentinel-3 SLSTR – SARP – Report 2 – 20th May 2020	FMI: Pekka Kolmonen, Larisa Sogacheva, Timo Viranen, Antti Lipponen EUMETSAT Technico Officer (TO) : Julien Chimot
RD-3	EUMETSAT – Atmospheric Aerosol Optical Depth retrieval performance from Sentinel-3 SLSTR – SARP – Report 3 – 25th March 2021	FMI: Kolmonen, Larisa Sogacheva, Timo Virtanen, Antti Lipponen, Timo Virtanen EUMETSAT Technico Officer : Julien Chimot
RD-4	Optimized Simultaneous Surface-Atmosphere Retrieval from Copernicus Sentinel-3 (OSSAR-CS3) - Product Validation Report (PVR), v1.0	EUM/SEN3/DOC/21/1244474 Written by Julien Chimot (EUMETSAT), 14.10.2021.
RD-5	Sentinel 3B SLSTR RAL Phase E1 In-Orbit Commissioning Report	S3-RP-RAL-SL-125
RD-6	Copernicus Sentinel-3 Product notice SLSTR Level-2 NRT AOD	EUM/SEN3/DOC/21/1249242v.1.0 Written by J. Chimot 14.10.2021.

1.4 Terminology

Acronyms and Abbreviations

Acronym/Abbr.	Explanation
AATSR	Advanced Along Track Scanning Radiometer
ACES	Aerosols Copernicus EUMETSAT Swansea
AFRI	Aerosol Free Ratio Index
AMV	Atmospheric Motion vector
ATSR	Along Track Scanning Radiometer
AAOD	Absorbing Aerosol Optical Depth
AOD	Aerosol Optical Depth
BC	Baseline Collection
CalVal	Calibration & Validation
CAMS	Copernicus Atmospheric Monitoring Service

Acronym/Abbr.	Explanation
AATSR	Advanced Along Track Scanning Radiometer
ACES	Aerosols Copernicus EUMETSAT Swansea
AFRI	Aerosol Free Ratio Index
AMV	Atmospheric Motion vector
ATSR	Along Track Scanning Radiometer
AAOD	Absorbing Aerosol Optical Depth
CCI	Climate Change Initiative
CLA	Cloud & Aerosol
DB	Deep Blue
DT	Dark target
EC	European Commission
ECMWF	European Centre for Medium-Range Weather Forecasts
ESA	European Space Agency
EUMETSAT	European operational satellite agency for monitoring weather, climate and the environment from space
FAQ	Frequently Asked Questions
FMAOD	Fine Mode Aerosol Optical Depth
FMF	Fine Mode Fraction
FMI	Finnish Meteorological institute
IPF	Instrument Processing Facility
L1B	Level 1B
L2	Level 2
L3	Level 3
LEO	Low Earth Orbit
LUT	Look-Up-Table
METIS	Monitoring 7 Evaluation of Thematic Information from Space
NDVI	Normalized Difference vegetation Index
NIR	Near InfraRed
NRT	Near Real Time
NTC	Non Time Critical
OLCI	Ocean & Land Colour instrument
OSSAR-CS3	Optimized Simultaneous Surface Aerosol Retrieval for Copernicus Sentinel-3
PB	Processing Baseline
PDF	Product Data Format
PN	Product Notice
QWG	Quality Working Group
RAD	Relative Azimuth Difference
RGB	Red-Green-Blue
RSP	Remote Sensing Products
RT	Radiative Transfer
RTM	Radiative Transfer model
S3	Sentinel-3
S3MPC	Sentinel-3 Mission Performance Centre
S3-NG	Sentinel-3 New-Generation
SARP	SLSTR Aerosol Retrieval Performance

Acronym/Abbr.	Explanation
AATSR	Advanced Along Track Scanning Radiometer
ACES	Aerosols Copernicus EUMETSAT Swansea
AFRI	Aerosol Free Ratio Index
AMV	Atmospheric Motion vector
ATSR	Along Track Scanning Radiometer
AAOD	Absorbing Aerosol Optical Depth
SLSTR	Sea & land Surface Temperature Radiometer
SSA	Single Scattering Albedo
SSAR	Simultaneous Surface Aerosol Retrieval
SST	Sea Surface Temperature
SU`	Swansea University
SWIR	Short Wave-Infrared
SZA	Solar Zenith Angle
TCWV	Total Column Water Vapour
TIR	Thermal InfraRed
TO	Technico Officer
UV-Vis	UV-Visible
vs.	versus
VZA	Viewing Zenith ANgle
w.r.t.	with respect to
WMO	World Meteorological Organization

2 EUMETSAT & COPERNICUS SENTINEL-3

2.1 EUMETSAT

EUMETSAT is an intergovernmental organisation established in 1986, which today provides 30 Member States with weather and climate-related satellite data, images and products – 24 hours a day, 365 days a year.
The primary objective of EUMETSAT is to establish, maintain and exploit European systems of operational meteorological, ocean, atmospheric composition, and climate satellites, taking into account as far as possible the recommendations of the World Meteorological Organization (WMO). The data generated by EUMETSAT's satellite systems and the derived products are supplied to the National Meteorological Services of the organisation's Member States in Europe, as well as to other users world-wide. A further objective of EUMETSAT is to contribute to the operational monitoring of the climate and the detection of global climate changes.
More detailed information about EUMETSAT and its organisational structure can be found at http://www.eumetsat.int.

2.2 Sentinel-3 & SLSTR

As part of the Copernicus programme, funded by the EC, S3 is the third of the Sentinel satellite series, originally dedicated to land and ocean applications including sea-ice, water pollution monitoring in open-ocean and coastal areas, surface temperature, sea height, and vegetation productivity. The mission provides continuity to the observations from the previous European Remote Sensing (ERS), Envisat and 'Satellites Pour l'Observation de la Terre' (SPOT) space-borne missions. The first satellite, S3A, has been flying since 16 February 2016. The second satellite, S3B, was successfully launched on 25 April 2018. Sentinel-3 is a Low Earth Orbit (LEO) mission; its orbit has a mean altitude of 815 km, is sun-synchronous with an ascending equatorial crossing local time of 10:00 am.

The potential of S3 to provide atmospheric products was acknowledged by the EC User Forum in 2015. SLSTR is a conical scanning imaging radiometer employing the along-track scanning dual-view technique (see Figure 1) to measure the radiance at the top of the atmosphere in nine spectral channels: six solar channels from the visible (554 nm) to the Short Wave-Infrared (SWIR) (2.25 µm), and three in the thermal infrared (, 375, 10.85 and 12.02 µm). Each scene is observed twice: in nadir and oblique backwards views. SLSTR is an evolution of the Along Track Scanning Radiometer (ATSR) series and Advanced Along Track Scanning Radiometer (AATSR) with a wider swath (1420 km in nadir, 750 km in backwards view) and an increased spatial resolution (~500 m near nadir viewing).

One of the major geometry configuration differences between the (A)TSR instruments and SLSTR is the viewing direction of the oblique view: while the (A)TSR oblique view was pointing to forward direction w.r.t. the satellite motion, the SLSTR oblique view is now pointing to the backward direction w.r.t the satellite motion (respectively South and North on the descending part of the satellite orbit). Additional significant differences include large extension of the swath width for both views, and two additional spectral channels in the Short Wave InfraRed (SWIR) at 1.37 & 2.25 µm (see Table 1).

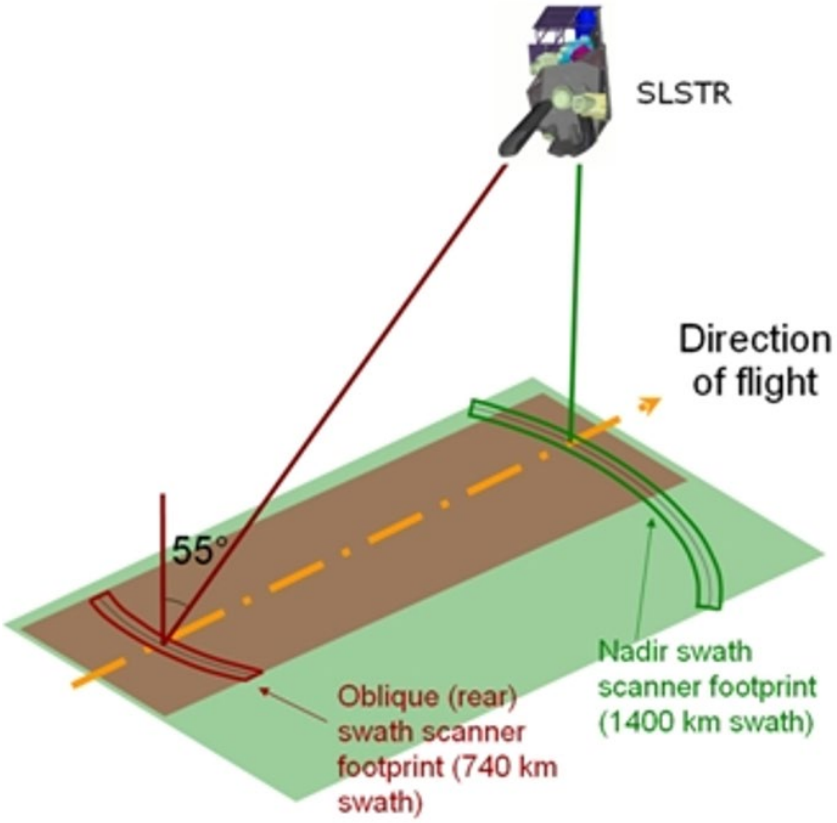

Figure 1: SLSTR dual-view configuration

SLSTR Band names	Wavelengths
S1 – Green	554 nm
S2 – Red	660 nm
S3 – NIR	868 nm
S4 - SWIR	1.374 µm
S5 - SWIR	1.61 µm
S6 - SWIR	2.25 µm

Table 1: SLSTR Solar spectral bands

3 CONTEXT: EUMETSAT/COPERNICUS MANDATE, REQUIREMENTS, AND CAMS

3.1 Operational Sentinel-3 (S3) Atmosphere Level 2 (L2) portfolio

The Copernicus Setinel-3 mission portfolio primarily includes the core products supporting the marine and land surface applications with responsibilities organized between EUMETSAT and the European Space Agency (ESA) as follow (see Figure 2):

- The operational Level 1B (L1B) optical measurements under joint responsibilities by both EUMETSAT & ESA ground-segments;
- The operational L2 marine portfolio exclusively procured under EUMETSAT responsibility
- The operational L2 land portfolio exclusively procured under ESA responsibility.

Since 2020, the operational S3 Atmosphere portfolio is added as the ensemble of official L2 atmospheric products & associated operational processors primarily explicitly dedicated to atmospheric users & services, but in principle publicly available & exploitable by anyone. This portfolio includes contributions from both agencies, EUMETSAT & the European Space Agency (ESA).

In line with its diverse mandates, EUMETSAT has the exclusive responsibility of leading a large series of components of the operational Sentinel-3 Atmosphere L2 portfolio:

- On-behalf of the European Commission (EC):
    - Optimized Simultaneous Surface-Aerosol Retrieval for Copernicus Sentinel-3 (OSSAR-CS3) in NRT https://www.eumetsat.int/S3-AOD
    - Optimized Fire Radiative Power for Copernicus Sentinel-3 (OFRP-CS3) in NRT https://www.eumetsat.int/S3-NRT-FRP to further constraint the sources of smoke and their long-range transport in the atmosphere.

- On-behalf of the EUMETSAT Member States, a a large series or new operational L2 atmospheric products are intended & under preparation, encompassing
    - OLCI Cloud Top Pressure from the O_2-A bands (OCTPO2) https://www.eumetsat.int/S3-OLCI-CTP
    - SYNergy Cloud Mask (SYN-CM) https://www.eumetsat.int/S3-synergy-cloud-mask
    - The OLCI Total Column Water Vapour (TCWV) based on the Near InfraRed (NIR) channels and the novel COWA algorithm https://www.eumetsat.int/COWA
    - The SLSTR dual-view Thermal InfraRed (TIR) TCWV from the AIRWAVE algorithm https://www.eumetsat.int/AIRWAVE-SLSTR
    - The SLSTR Atmospheric Motion vector (AMV) (Barbieux *et al.*, 2021).

It is emphasized that the OSSAR-CS3 & OFRP-CS3 processors are unique EUMETSAT/Copernicus procurements, independent, and with significant differences from any other operational or research aerosol and fire algorithms existing from research institutes and/or space agencies (*e.g.* ESA). Although some consistencies may be found, users are advised to bear in mind their various differences in terms of product format & content, algorithm, and processor capabilities.

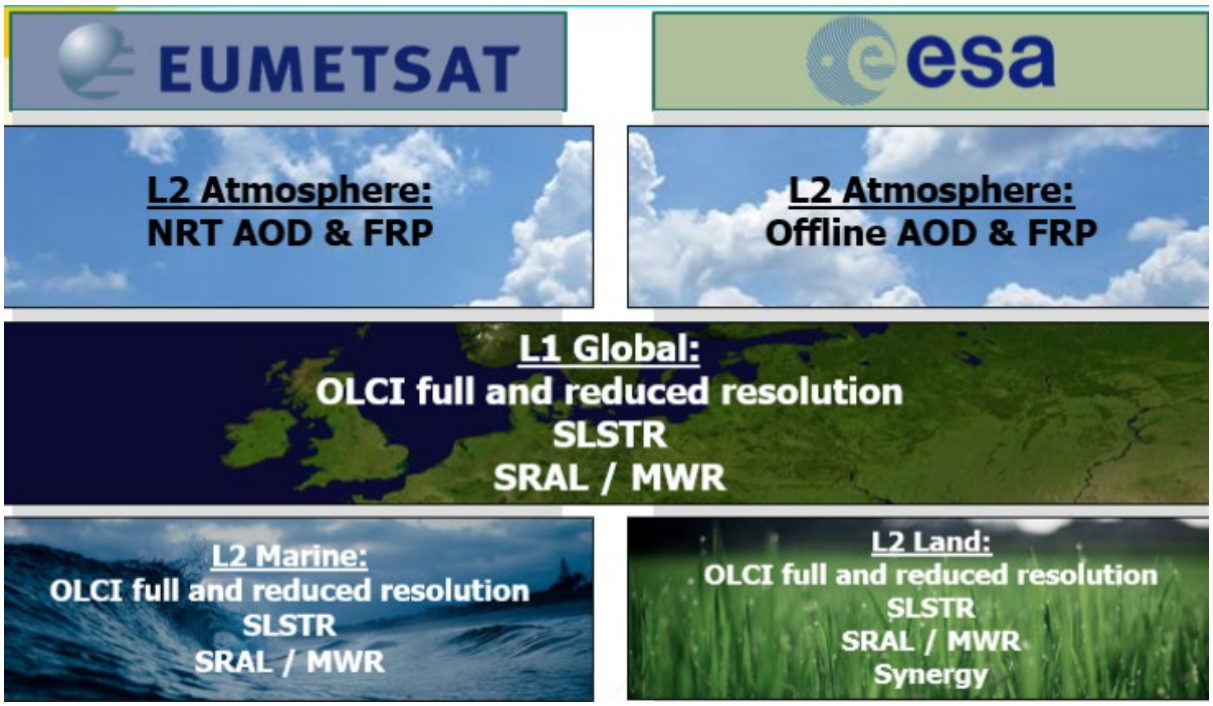

Figure 2: Organisation of procurements & responsibilities on the operational Sentinel-3 products between EUMETSAT & ESA.

3.2 What is the OSSAR-CS3 product?

The European Commission (EC) mandate, exclusively entrusted to EUMETSAT, covers leading & procurement of:

- The operational Sentinel-3 L2 aerosol product
- As an integral part of the Copernicus program
- In NRT timeliness: *i.e.* available to any users in no more than 3h strictly starting from the instrument sensing time
- A high scientific expertise to support all operational users, agencies, and services for a satisfactory exploitation in a timely manner compatible with the NRT scientific requirements.
- Complete validation & operational quality monitoring
- Partial reprocessing to ensure long-term quality and stability requirements with respect to (w.r.t) instrument & L1 product evolution.
- Specification, prototyping & implementation of algorithm & processor baseline as well as any evolutions.

The OSSAR-CS3 is the reference processor led by EUMETSAT resulting from this mandate and generating & disseminating the associated product to meet all the specified European requirements, both operational & scientific. It is supported by contributions from various partners involved at different stages of the development (see Sect. 1.1). OSSAR-CS3 is also intended to be operationally exploited by the Copernicus Atmospheric Monitoring Service (CAMS).

The various optimization performed behind this product covers a broad range of aspects:

- Operational to ensure continuous and stable production as well as dissemination to all public users with very low interruption.
- Timeliness to guarantee the availability in an effective timely manner to all operational institutions & services.
- Scientific to cover all user needs & operational atmospheric service requirements in spite of the natural challenges imposed by the operational & timeliness requirements above.
- Continuous evolutions whenever necessary to ensure the processing benefits from up-to-date scientific knowledge related to aerosols but also Level 1B (L1b) spectral measurement quality as well as the instrument performance.

Feedbacks from independent expert users, the European Commission (EC), operational services, and EUMETSAT member state scientific & technical delegates are regularly included *via* new prototyping developments & updates or evolutions of the operational processor.

3.3 Monitoring, forecasting and analysing our atmosphere composition — the Copernicus Atmosphere Monitoring Service (CAMS)

Implemented by the European Centre for Medium-Range Weather Forecasts (ECMWF) on behalf of the European Commission (EC), the Copernicus Atmosphere Monitoring Service (CAMS) will be one of the key users of the Copernicus Sentinel-3 NRT AOD product. CAMS provides continuous data and analysed information on atmospheric composition. This service globally analyses the current air quality in NRT, forecasts the situation a few days ahead, and consistently analyses retrospective data records for recent years, hence enabling a permanent assessment of the air quality that we breathe. It supports many applications in a variety of domains encompassing health, environmental monitoring, renewable energies, meteorology, and climatology. Five main areas are focused by the service: 1) air quality and atmospheric composition, 2) ozone layer and Ultra-Violet (UV) radiation, 3) emissions and surface fluxes, 4) solar radiation, 5) climate forcing. Daily global atmospheric composition relies on the forecasting of constituents such as reactive and greenhouse gases, ozone and aerosol particles.

To optimise the boundary quality of the forecasts, observations are assimilated and satellites are one of the main providers. Today, MODIS sensors on-board Terra and Aqua satellites procured by the National Aeronautics and Space Administration (NASA) and the Polar Multi-sensor Aerosol optical Properties (PMAP) from the Metop satellites procured by EUMETSAT are the operational aerosol observations assimilated by CAMS. In future, additional satellite aerosol observations will be added in the CAMS system including the NASA Suomi Visible InfraRed Imaging Radiometer (VIIRS) and the Copernicus Sentinel-3 NRT AOD *via* the OSSAR-CS3 processor.

3.4 Our understanding of the operational aerosol user requirements

EUMETSAT is already leading since 2014 the procurement of the operational NRT Polar Multi-Sensor Aerosol product (PMAp) from the 3 European Metop A-B-C satellites. This product results from a complete synergy (spectral & geometry) of 3 sensors: AVHRR, IASI, and GOME-2. OSSAR-CS3 is hence not the first, but the 2nd operational NRT European aerosol product.

Both OSSAR-CS3 & PMAP benefit from long-term EUMETSAT & external European aerosol experts for the benefits of the large aerosol community, especially operational air quality & climate services, meteorological agencies, and other R&D institutes. CAMS is one major application of these products to understand the immediate and long-term impact of aerosol particles on our air quality, Earth radiation, and changing climate. As such, EUMETSAT regularly implements all necessary evolutions such that OSSAR-CS3 & PMAP provide consistent information w.r.t. the American operational aerosol satellite constellation composed of MODIS Terra, MODIS Aqua, VIIRS/SNPP & VIIRS NOAA-20.

Based on feedback from our long-term operational aerosol product, but also various published documents, the AOD requirements at 550 nm (the standard wavelength commonly used in the aerosol community) is understood to be the most crucial aerosol parameter to be provided and as a consequence, it should be our 1st priority. This parameter is absolutely critical and needed by operational air quality services such as CAMS. CAMS has expressed through multiple exchanges (e.g. communication with EUMETSAT and the EC in the context of S3 & the future S3-New Generation, S3-NG), the following requirements:

- A precision better than 10% or 0.03, whichever is larger (target; 15% or 0.05, threshold).
- An accuracy better than 10% or 0.03 whichever is the largest (target; 15% or 0.05, threshold). This requirement is very similar to the original GCOS requirements(see RD-4).

These key requirements on AOD(550 nm) have to be combined with the following:

- Precision & accuracy requirements shall be applicable as much as possible globally, and not to a restricted geographical area.
- Horizontal resolution shall lie within the range of 5:10 km.
- *A posteriori* AOD(550 nm) uncertainty shall be predicted & provided per individual AOD pixel.
- The operational AOD parameter shall be made available as input to the operational services in no more than 3h since the sensing time. Hence, optimized timeliness is a critical component of any operational satellite aerosol products.

After the AOD(550 nm) needs are satisfied, there are emerging needs from operational users on additional aerosol parameters such as: AOD at multiple spectral wavelengths, AOD uncertainty, and all parameters referring to particle properties (fine mode, absorption, size, altitude, etc…). Several of these parameters are today produced from the OSSAR-CS3 processor but have benefited of a lower priority compared to the AOD(550 nm) during its development phase. They will however be consolidated in a near-future.

4 THE OSSAR-CS3 PROCESSOR: HISTORY, INPUTS, PRE-PROCESSING, AND OUTPUTS

4.1 Product Processing Baseline History & Quality labels

The 1st operational deployment of the OSSAR-CS3 processor in the EUMETSAT Sentinel-3 ground-segment was in August 2020 leading to the very first version of the Copernicus S3 Aerosol NRT product publicly available as well as its reprocessed series. The following nomenclature is associated:

- Instrument processing Facility (IPF) v2.0
- Baseline Collection (BC) 1
- Processing baseline (PB) 1.0.

Explanation about the nomenclature:

- The PB overall includes the product BC, IPF version, and version of static auxiliary data files.
- The BC 1 is clearly indicated in the SAFE directory name as the last three digits ("*001*") before the extension *.SEN3*.
- The used IPF version is indicated in the Global Attributes of the product netcdf file (*NRT_AOD.nc*).

The product quality label associated with PB 1.0 was:

- Over **ocean surfaces,** the quality label is '**Preliminary Operational**'. Its scientific quality is considered to be approaching the expected requirements, nevertheless it is considered to have reached a level of maturity which can be safely exploited by users. To confirm the final operational status validation is being performed over longer time series with a larger set of ground-based measurements, with fine-tuning continuing for the evolution to the full 'operational' maturity level, *i.e.* matching the expected quality requirements, within the year.
- Over **land surfaces**, the quality label is '**Demonstrational**' as this has been the very first release of this parameter and its product quality is not yet within the expected requirements. It is noted that in this case it should be used with caution noting its known current limitations. The associated novel algorithm has been still the subject of further improvements & optimisation by EUMETSAT.

Since 28th October 2021, a new version is operationally deployed as follows:

- Instrument processing Facility (IPF) v3.0
- Baseline Collection (BC) 2
- Processing baseline (PB) 2.0.

This version includes major improvements of the product over land surfaces (see [RD-4] & [RD-6]). As a result, the quality label of over **land surfaces** is upgraded to '**Preliminary Operational**', and is hence aligned with its over ocean surfaces counterpart.

For further information, users are strongly advised to read the Product Notice (PN) [RD-6] on the EUMETSAT website dedicated to Copernicus Sentinel-3 atmospheric composition: https://www.eumetsat.int/atmospheric-composition.

4.2 Inputs & pre-processing

The key input of OSSAR-CS3 is the SLSTR Level 1 B (L1B) product exclusively procured in NRT, containing not only the SLSTR L1B radiances at fine resolution (500 m) in the Solar bands as well as the meteorological forecasts (wind, gases, etc…) produced by ECMWF. The following pre-processing is then performed:

- Verification of the quality of each L1B pixels based on the quality indicators given by the SLSTR L1B product. Al invalid measurements are by default excluded.
- Identification of land & sea L1B fine pixels based on the SLSTR L1B surface mask.
- *A priori* cloud detection at fine resolution for each pixel, in each nadir & oblique view, based on the SLSTR L1B basic cloud mask. While over ocean, the full L1B cloud mask is considered, only the L1B TIR cloud tests are read over land surfaces (see Sect. 7.1.3).
- The aerosol retrieval is not performed at the l1B fine resolution, but at a coarser resolution to smooth "system" noise (see Sect. 7.1.8). The so-called L2 aerosol super-pixel is the aggregation of the original cloud-free and reliable L1B TOA radiances for both nadir & oblique views at the desired L2 resolution. A super-pixel is considered as valid for aerosol retrieval attempt is the resulting cloud fraction is lower or equal to 50%.

4.3 Outputs

The overall product output is the ensemble of parameters characterizing aerosol & surface properties over land and ocean surfaces at the requested L2 resolution:

- Multi-spectral AOD: all values (*i.e.* non *a posteriori* filtered out), and best values (*a posteriori* filtered – see Sect. 7.1.9).
- *A posteriori* AOD(550 nm) uncertainty: all values (*i.e.* non *a posteriori* filtered out), and best values (*a posteriori* filtered – see Sect. 7.1.9).
- Angstrom exponent(550 – 865 nm).
- Multi-spectral Single Scattering Albedo (SSA).
- Multi-spectral directional surface reflectance.
- Absorbing AOD(550 nm) (AAOD).
- Dust AOD(550 nm).
- Fine Mode (FM) AOD(550 nm).
- Latitude & longitude coordinates of teh centre of teh L2 pixel
- Geometry parameters for each nadir & oblique views: Solar Zenith Angle (SZA), Viewing Zenith Angle (VZA), Relative Azimuth Difference (RAD), scattering angle.

5 HISTORY & SCIENTIFIC BACKGROUND

5.1 History & scientific teams

The **algorithm baseline behind the OSSAR-CS3 processor** is a **joint prototyping development between EUMETSAT & SU**. The key involved teams have been:

- SU: the team led by Prof. Dr. Peter North from the Geography department.
- EUMETSAT: the Cloud & Aerosol (CLA) scientific team within the Remote Sensing Products (RSP) division, led by Dr. Bertrand Fougnie, with ideas & developments overall led by Dr. Julien Chimot.

A key goal by EUMETSAT is to establish a high degree of resiliency to any past & future changes in the dual-view direction for ensuring a consistently high quality over all geographical areas (*i.e.* global.).

The starting point is the original aerosol dual-view algorithm as imagined by Prof. Dr. Peter North from SU, firstly applied to the European Space Agency (ESA) Along-Track Scanning Radiometer-2 on-board ERS-2 (North *et al.*, 1999, 2002b). This first prototype was then much further developed and applied to the ESA Advanced AATSR (AATSR), a direct successor of ATSR-2, on-board the ENVISAT Earth satellite (2002-2012). This algorithm was notably funded by the ESA aerosol Climate Change Initiative (CCI) project https://climate.esa.int/en/projects/aerosol/. Later on, it was slightly adapted to new SLSTR channels & associated spectral response functions leading then to the SLSTR SU prototype v1.0 (see Sect. 6).

The original design of the SLSTR aerosol algorithm comes from the SU SLSTR prototype v1.0. This version is overall very close to the past developments achieved for the ESA ENVISAT/AATSR sensor with the following minor differences:

- Addition of the SLSTR S6 (2.25 µm) spectral channel both over ocean (spectral) and land (joint dual-angular surface & aerosol)
- Look-Up-Tables (LUTs) generation specific to the actual SLSTR spectral measurements:

This algorithm was then converted into a 1st version of the processor, labelled as Instrument Processing Facility (IPF) v1, which is the precursor of the actual OSSAR-CS3 IPF running today in the EUMETSAT S3 ground-segment. The precursor IPF was developed by the Copernicus S3 Mission Performance Centre (S3MPC), *via* the company ACRI-ST, and procured by ESA. After delivery to EUMETSAT in October 2018, the precursor IPF v1.0 was never operationally deployed but rather went under various modifications & an in-depth redesign based on new prototyping developments procured under EUMETSAT leadership. These are detailed in the next Sect. 7.

To anticipate not only the specificities of SLSTR but also the new constraints related to the operational scientific requirements, EUMETSAT, SU & FMI have reanalysed in-depth the actual aerosol-surface information content offered by any dual-view radiometers with a special focus on the importance of the dual-view geometry (regardless of their actual oblique view orientation) for a performant operational, global & daily processing. This has led to the identification of some gaps in the original SLSTR algorithm baseline. As a consequence, in

line with its own mandate and benefiting from expertise & outcomes from analysis, EUMETSAT has decided to specify and develop a series of new developments deemed as critically needed to accommodate with the new context (see Sect. 7). The main motivation has been to ensure the compliancy with the EUMETSAT requirement for operational scientific quality and in line with its scientific roadmap for aerosol developments [RD-1]. These additional developments have been prototyped, and implemented in-house in the new operational processor version v2.0. They are overall combined with several of the pre-existing components offered by the precursor SU prototype algorithm v1.0.

This evolved algorithm, jointly developed between SU and EUMETSAT, is the reference baseline supporting the OSSAR-CS3 processor since its 1st public NRT deployment in the operational EUMETSAT S3 ground-segment in August 2020.

NB: This algorithm baseline as described in all the next sections is associated with the latest Product Processing Bassline (PB) 2.0 – Baseline Collection (BC) 2 – Instrument Processing Facility (IPF) v3.0. Although several latest ideas and technical works come from EUMETSAT, others were strongly inspired thanks to direct supports provided by Prof. Dr. P. North (SU) during his visits in Darmstadt during 2019, to understand the original SU algorithm v1.0 structure.

5.2 Theoretical background

Everywhere on Earth, particles are suspended in the air, with a high regional and temporal variability, and threaten our air quality. Air pollution is a long-running global problem, sometimes named the 'silent killer'. Tiny particles suspended in the air, known as 'Particulate Matter' (PM) are one of the major environmental causes of disease around the world. In particular, PM2.5 (PM of less than 2.5 µm size) is a key health risk factor in Europe, above others, such as noise, ozone, or radon (Hanninen and Knol, 2011). Atmospheric aerosols are small and complex chemical mixtures of liquid and particles suspended in the air. Due to their tiny dimensions, they are usually invisible to the human eye at low concentration. However, they efficiently interact with solar radiation and strongly affect its distribution throughout the atmosphere (Dubovik et al., 2019). Their presence perturbs our climate system, total atmospheric energy budget, atmospheric visibility, human health and safety. Scattering and absorption by aerosols affect the actinic flux, and consequently modifies the photolysis rates of important processes in the atmosphere (Palancar et al., 2013). Furthermore, because of their interaction with the solar, Earth, and atmospheric radiations, aerosols also interfere with satellite observations dedicated to many applications such as air quality, climate and surface applications.

Aerosols differ from gases as they are bigger than molecules. There are several classifications of atmospheric aerosols but the most widely used is according to their size. They range from the smallest superfine mode, with diameters of a few nanometers (nm), to large coarse mode particles, with diameters to more than 100 micrometers (µm) or more. Between the superfine and the coarse mode particles are the fine mode particles, with diameters ranging from 0.1 mm to a few µm (Seinfeld, 1986). In polluted conditions, they are often denoted as particulate matter (PM): *e.g.* PM10 referring to the dry mass of particles with a diameter less than 10 µm.

Aerosol sources combine both natural and anthropogenic processes, and are of two types:

1. Direct emission resulting from dispersion of material at the Earth surface (*e.g.* sea spray aerosol from sea surface or waves, dust from desert outbreak (see for example Figure 2), biomass burning aerosol, volcanic ash resulting from eruptions, primary organic aerosol, industrial debris).
2. Indirect emission resulting from chemistry transformation of precursor trace gas, released by anthropogenic activities at the surface, leading to the formation of secondary aerosols (*e.g.* sulfates, nitrates, ammonium salts, secondary organic aerosol).

There are still some gaps in our understanding and modelling of aerosol sinks (IPCC: The Core Writing Team Pachauri and Meyer, 2014). After their release, they undergo various physical and chemical processes modifying their size and optical properties. They are generally removed from the air by dry or wet depositions, depending on their size and Earth's surface characteristics, at the surface (Kerkweg *et al.*, 2006; IPCC: The Core Writing Team Pachauri and Meyer, 2014).

The global total atmospheric aerosol mass is dominated by natural processes at the surface, in particular sea spray aerosol and desert dust. However, anthropogenic emissions (*e.g.* industries, vehicles, agriculture and wildfires) of both primary particles and precursor gases greatly increases the total aerosol load and can locally outweigh the natural aerosols (Andreae and Rosenfeld, 2008).

The reasons to observe atmospheric aerosols are numerous:

- Aerosols directly influence the radiation budget of the Earth-atmosphere system through the scattering and absorption of solar and terrestrial radiation (Feingold *et al.*, 1999). High concentrations of fine particles lead to reduced cloud droplet size, enhanced cloud reflectance (Twomey *et al.*, 1984), and reduced precipitation (Rosenfeld, 2000; Ramanathan *et al.*, 2001; Rosenfeld *et al.*, 2002). Yet accounting for the effects of aerosol particles is very difficult since they represent one of the most complex atmospheric constituents. For example, it has widely been recognised that the lingering uncertainty in the knowledge of aerosol properties drives the global climate change estimation uncertainly (Dubovik *et al.*, 2019). These large uncertainties of aerosol optical properties limit our climate predictive capabilities (IPCC: Solomon *et al.*, 2007).
- Aerosols play a significant role in air quality, in particular near the surface. Due to the rapid growth of both population and economic activity, such as in the Asian region, increase in fossil fuel emissions gives rise to concerns about fine particles formation and dispersion. Aerosols include a variety of hazardous organic and inorganic substances, reduce visibility, lead to reductions in crop productivity and strongly affect the health of inhabitants in urban regions (Chameides *et al.*, 1999; Prospero, 1999; Eck et al., 2005). In its last report (Clear the air for children, October 2016), UNICEF has emphasized these striking numbers: globally, 1), 2 billion children live in areas where outdoor air pollution exceeds international limits, 2) 300 million children live in areas where outdoor air pollution exceeds six times international limits. The Americas and Europe are also concerned: 120-130 (20) million children live in areas where outdoor air pollution exceeds (twice) international limits (*cf.* UNICEF, 2016).

- In the absence of clouds, aerosols interfere with the signal of interest on every optical satellite observation from passive sensors. Taking into account such an interference is critical for many applications like surface ocean colour (e.g. from the Copernicus Sentinel-3 Ocean & Land Colour instrument (OLCI) L2 Ocean Colour product procured by EUMETSAT) or trace gas retrieval from any UV-Visible (UV-Vis) instrument.

5.3 Review of dual-view space-borne information content for the SSAR concept

After cloud filtering, the main challenge of retrieving aerosol properties from any satellite sensor (mono or multi-viewing) is the decoupling of aerosol scattering and surface reflectance. This is true for any surface type, although larger difficulties are usually encountered over lands, especially the so-called bright soils such as hybrid, urban, bare & deserts. Over such surfaces, land reflectance highly dominates the overall Top Of the Atmosphere (TOA) measurement. Decoupling aerosol-surface can be done either by using ancillary surface database, or *via* a Simultaneous Surface Aerosol Retrieval (SSAR). The advantage of the SSAR concept is to be as much as possible independent from any prior data uncertainties and to exploit the maximum information contained in the acquired measurements. In the absence of a polarimeter, a SSAR can only be achieved *via*:

- spectral constraints, assuming spectral land reflectance is known or can be easily determined. This usually requires not only a large spectral coverage (from deep blue to the short-wave infrared), and a very high radiometric and spectral calibration quality.
- or with geometry constraints: *i.e.* multi-viewing sensors that sample the same scene with different scattering angles and isolate directional components of both aerosol and land surface scattering. However, as explained in B. Fougnie *et al.* (2020), a large fraction of the aerosol phase function must be sampled to allow such a decoupling. The key reason is related to the dependency of both the aerosol & land surface signals on the sampled geometry: while aerosol signal dominates in forward direction: *i.e.* low scattering angle), land cover exhibits a larger signal in backward direction (see Figure 3).

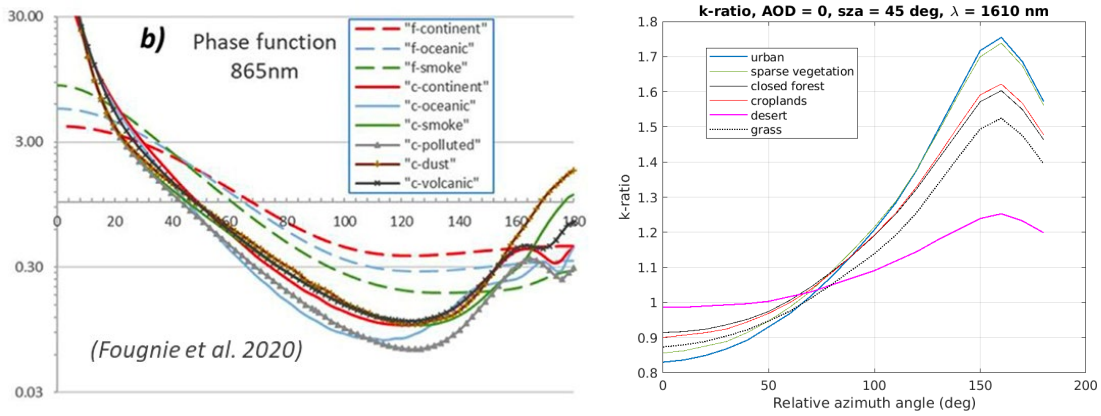

Figure 3: Geometry information content for the SSAR concept from space-borne measurements.

Left: aerosol phase function, for different aerosol models, vs. scattering angle at 865 nm (B. Fougnie *et al.*, 2020).

Right: SLSTR dual-view measurements ratio ("k-ratio) at 1.6 µm as a function of the oblique view relative azimuth angle (extracted from the EUMETSAT SARP project report – P. Kolmonen *et al.*, 2020 - [RD-2]).

A critical element to ensure the SSAR success is the careful consideration of the actual information content in the measurements:

- the higher is the information content, the higher is the capability to retrieve independently a large number of aerosol and surface parameters directly from the measurements;
- the lower is the information content, the higher is the need to consider external assumptions (or ancillary data) to better constraint surface signal contained in the sensor measurements.

The key advantages of SLSTR for aerosol retrieval are primarily a large spectral coverage covering visible – Near InfraRed (NIR) - SWIR. Secondly, its second view offers more observations than a traditional mono-viewing sensor (*e.g.* MODIS).

However, any dual-view sensors like SLSTR and (A)ATSR has drawbacks for an optimal application of the SSAR concept on an operational global – daily basis. The most critical challenge is the very limited number of views compared to real designed multiple viewing instruments such as 3MI on the future EPS-SG or POLDER/PARASOL. With only 2 views, only a limited range of the scattering angles (and, therefore, the phase function) will be sampled everywhere on Earth, regardless of the dual-view configuration/orientation (see Figure 4). While both forward and backward scattering reflectance (*i.e.* favourable geometry) will be sampled over some regions, other areas will always be measured in the so-called backward scattering (*i.e.* unfavourable geometry).

Furthermore, it is worth noticing that the dual-view configuration from (A)ATSR to SLSTR differs in two ways: 1) a rotation of 180 deg (*i.e.* the oblique view is now pointed backwards instead of forward w.r.t. the satellite motion), and 2) the extended width of both nadir & oblique views. While such a dual-view rotation has *a priori* no impacts on thermal infrared measurements and derived L2 products, such as Sea Surface Temperature (SST), it directly affects the spatial distribution of the viewing configuration associated with radiance measurements acquired within the solar bands. Therefore, the spatial distribution of their signals as measured by SLSTR is geographically modified. The so-called unfavourable geometry, *i.e.* both views only sample backward scattering measurements, is primarily located (see Figure 4):

- during summer: essentially in the north, roughly above 20 degrees south;
- during winter: essentially on the western side of the nadir and oblique swaths.

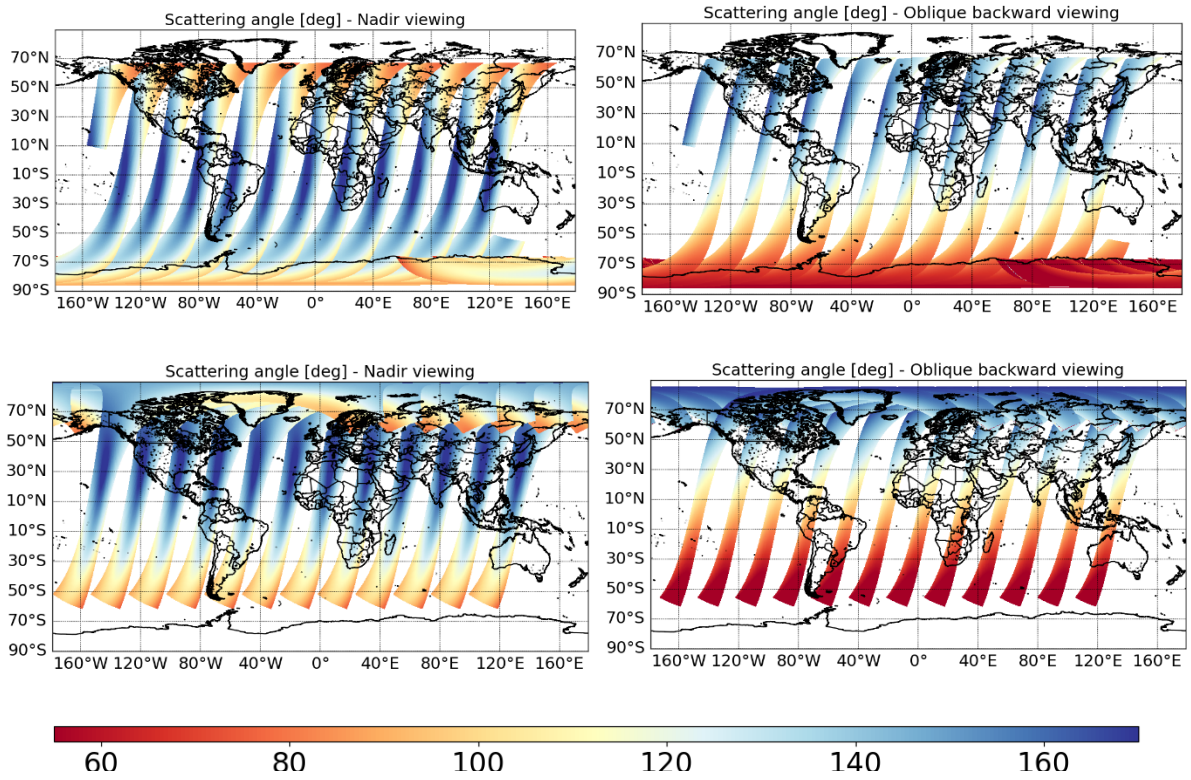

Figure 4: Scattering angle computed for the SLSTR nadir & oblique views separated for two specific days. Top: 1 day during winter. Bottom = 1 day during summer.

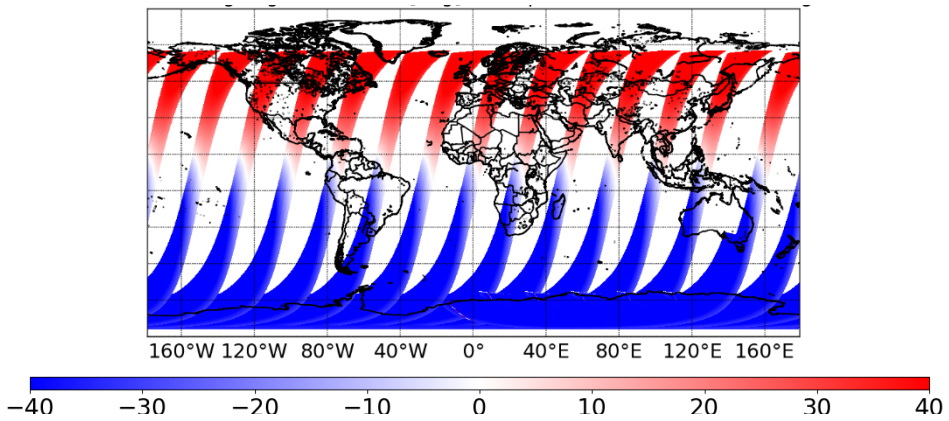

Figure 5: Scattering angle difference (in deg) between oblique & nadir SLSTR views – 1 day during Winter.

Moreover, regardless the oblique view direction, rearward as in SLSTR or forward as in (A)ATSR, the difference in the scattering angle values between both is always very low (less than 15 deg) in the latitude areas close to the Tropics (see Figure 5). In such regions, a dual-view system rarely brings sufficient additional geometry information compared to mono-viewing sensors.

Based on Figure 3, the favourable / unfavourable dual-view geometries are defined as follow:

- **If both views sample a scattering angle value higher than 110 deg**, the dual-view geometry is labelled as **unfavourable**.
- **If at least 1 view** (nadir and/or oblique) **samples a scattering angle value lower than 110 deg**, the dual-view geometry is labelled as **favourable**.
- NB: The difference in the scattering angles between both views as illustrated in Figure 5 is not exploited today. But it will be certainly important to further focus on them in the future, especially near the Tropics.

To understand the consequences of the geometry information content from any dual-view sensor, regardless of their oblique view orientation:

- Figure 6 illustrates the TOA reflectance with different AOD values simulated for the oblique view in two specific scattering angles (extracted from the EUMETSAT SARP project report – P. Kolmonen *et al.*, 2020 -[RD-2]).
- Figure 7 shows the spectral variability of the k-ratio of the dual-view reflectances (aerosol or land surface only) as a function of land cover estimated *via* the Aerosol Free Ratio Index (AFRI). The k-ratio is the ratio of the oblique view to the nadir view reflectance per individual wavelength (Veefkind *et al.*, 2000). AFRI is estimated as follows:

$$AFRI = \frac{RLand_{S3} - 0.5 * RLand_{S6}}{RLand_{S3} + 0.5 * RLand_{S6}}$$

With $RLand_{S3}$ & $RLand_{S6}$, the land surface reflectance in the S3 (0.8 µm), and S6 (2.25 µm) channels respectively. The AFRI allows to detect the nature of land cover (Karnieli *et al.*, 2000). It differs from the Normalized Differentiation Vegetation Index (NDVI) as the SWIR 2.25 µm is used instead of the red channel. The main reason is to avoid the large interferences caused by aerosols in the red while the far SWIR is mostly transparent to fine particles (a bit less to coarse particles such as dust however).

The following is interpreted & deduced:

- In favourable geometry, the dual TOA measurements will give access to both low and high aerosol signals, both low and high land surface reflectance. A large gradient will be observable across both nadir and oblique views. Furthermore, while a strong spectral feature will be visible in the aerosol signal across the dual-view, none to low spectral feature will be observable for the surface reflectance. This means that the surface colour will remain pre-dominantly similar across both views over mo land cover types.
- In unfavourable geometry: the dual TOA measurements are exclusively dominated by the effective bright surface (*e.g.* vegetation hotspot). The relative aerosol signal is usually much weaker in both views. Furthermore, while the aerosol signals across-both views will be spectrally quite similar (and lower), land covers with a high vegetation density can depict high spectral changes between nadir and oblique views. Desert, bare & hybrid (low vegetation) soils are expected to show lower spectral variation across both-views however. This is probably due to their nearly close Lambertian geometry properties, while well-developped vegetation is known to display a strong geometry

asymmetry (*i.e.* bright spot in backward direction – See Figure 3). While the first difficulty will be primarily caused by the enhanced surface brightness signal, the variable spectral features in the land vegetation geometry by opposition to aerosols is expected to add another significant challenge.

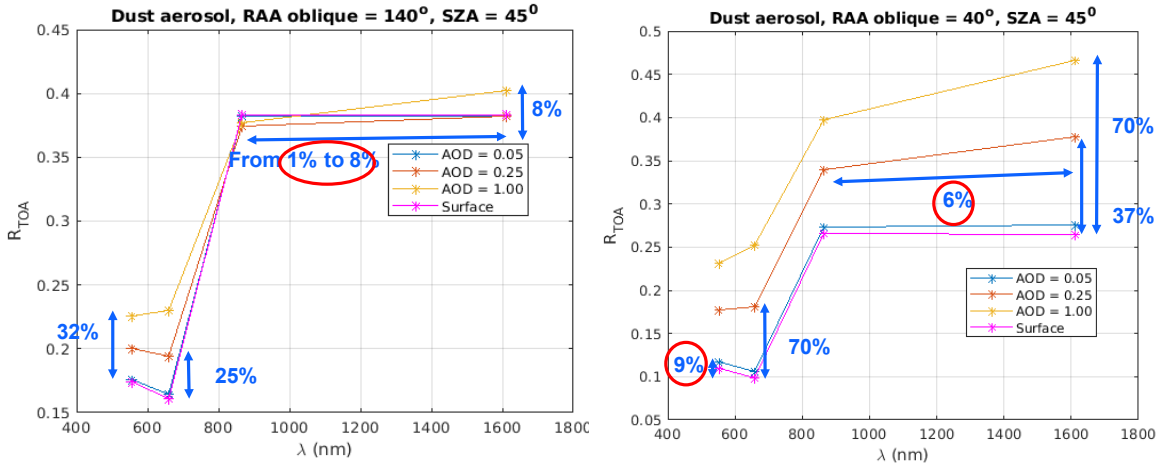

Figure 6: SLSTR simulated TOA reflectance within the oblique view for dust aerosol, with variable AOD(550 nm) values, in two different geometries. Lef: backward geometry (high scattering angle) Right: forward scattering (*i.e.* low scattering angle) (extracted from the EUMETSAT SARP project report – P. Kolmonen et al., 2020 -[RD-2]).

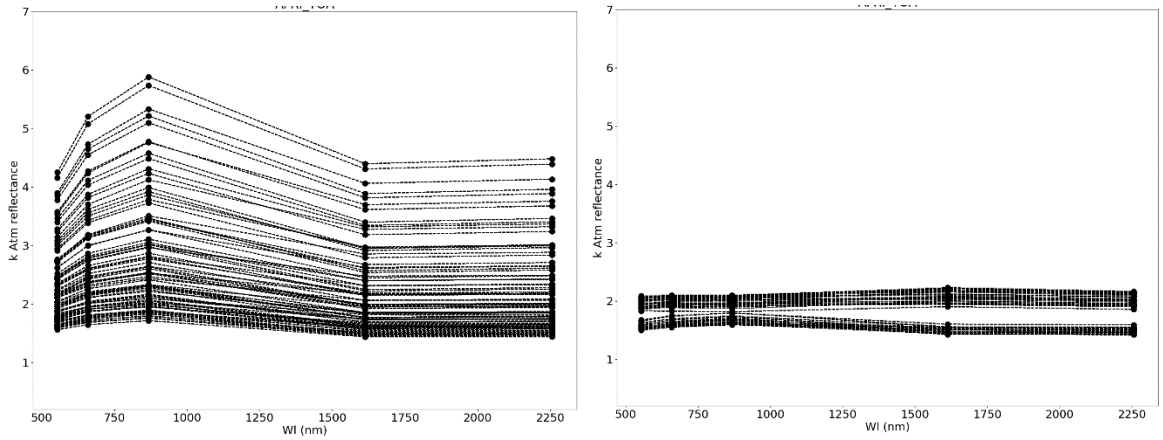

Figure 7: Spectral k-ratio for the atmospheric reflectance (aerosols + Rayleigh). Left: Low theta, Right: high theta.

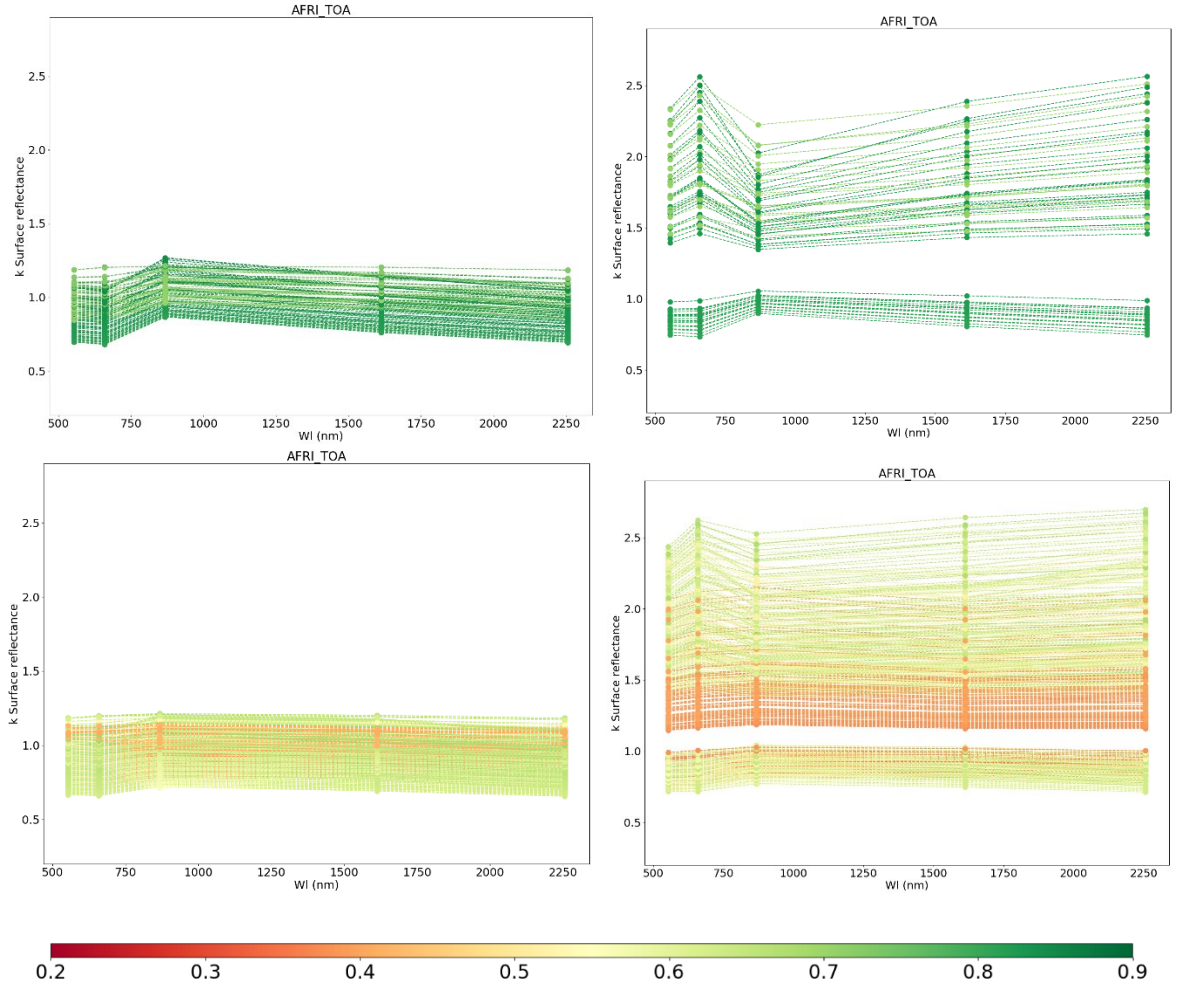

Figure 8: Spectral k-ratio for the surface reflectance (aerosols + Rayleigh removed). Left: favourable dual-view geometry), Right: unfavourable dual-view geometry – Note that lines at the bottom correspond to cases in which the scattering angles are nearly similar (difference lower than 20 deg) between both views.

In addition to the limited number of views, other challenges from SLSTR are: 1) the lack of blue channels allowing to acquire more information about aerosol absorption magnitude while strongly reducing land surface brightness 2) the lack of polarisation measurements that could give extra information on particle size and fine mode, and 3) the lack of (di)oxygen-A (O_2-A) for deriving information about scattering layer height.

Since operational users require global coverage for AOD(550 nm), and the geometry information content is crucial but very heterogeneous, an exclusive use of geometry constraints in a SSAR concept applied to any dual-view space-borne measurements is never globally enough, regardless of the actual dual-view orientation (backward of forward). Consequently, an operational SSAR processing with SLSTR requires additional constraints to optimize an efficient aerosol-surface decoupling with a global daily coverage, with special emphasize on land covers associated with medium & high vegetation density sampled in unfavourable dual-view geometry (see Figure 31 & Figure 32). Since there are not always everywhere enough information content from the acquired dual-view measurements, *a priori* assumptions on the surface signals are considered in OSSAR-CS3 (see Sect. 7.1.2 & 7.1.5).

6 ORIGINAL SU AEROSOL SLSTR ALGORITHM BASELINE

6.1 The iterative optimization scheme

The original aim of the SU prototype v1.0 is to make use of the angular and spectral sampling available from SLSTR to allow aerosol retrieval over land and ocean. The problem is formulated as one of optimisation subject to multiple constraints, which has been widely applied to atmospheric retrievals (Dubovik, 2005). Figure 9 illustrates the retrieval framework. The two-stage optimization process is employed: (1) Given a set of satellite TOA radiances, and an initial guess of atmospheric profile, we estimate the corresponding set of surface reflectance. (2) Testing of this set against a constraint results in an error metric, where a low value of this metric should correspond to a set of surface reflectances (and hence atmospheric profile) which is realistic. Step (1) is repeated with a refined atmospheric profile until convergence at an optimal solution. Two parameters describing the aerosol content are directly retrieved during the inversion: AOD at 550nm (τ550) and fine mode fraction, while further aerosol parameters are constrained by a climatology giving likely seasonal and spatial sources of aerosol. The algorithm components are therefore (i) design of an efficient and accurate scheme for deriving surface reflectance for known atmospheric profile, (ii) formulation of constraints on the land surface reflectance suitable for SLSTR, and (iii) iterative inversion scheme to retrieve the free aerosol parameters.

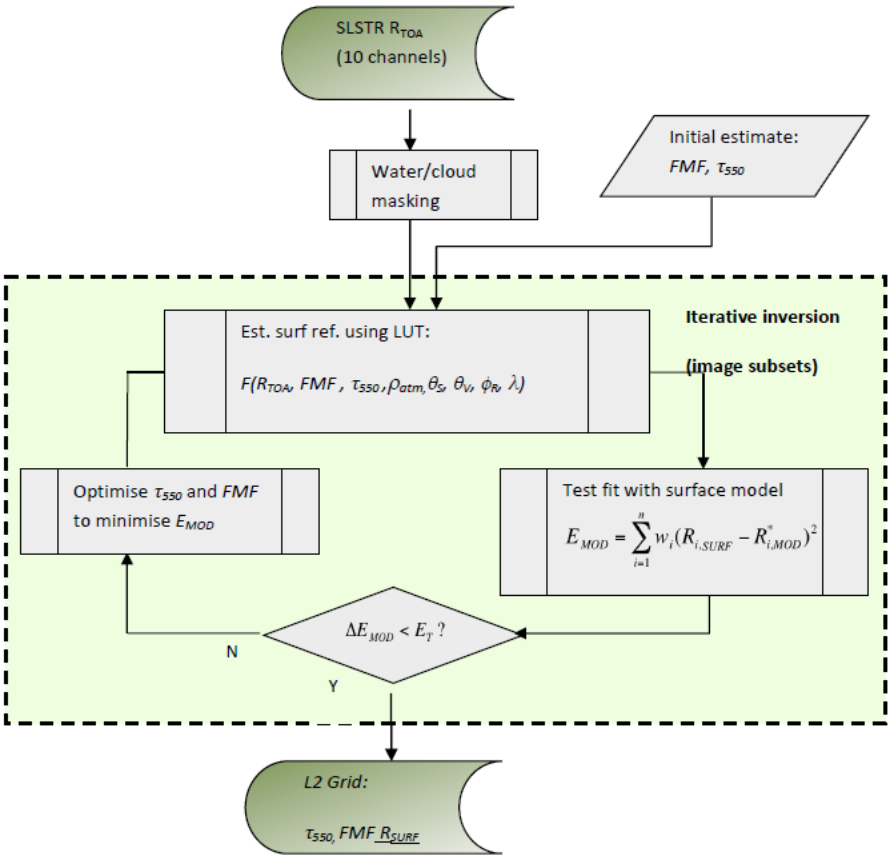

Figure 9: Algorithm baseline for simultaneous surface-aerosol properties (τ and FMF) from SLSTR data. The principle baseline is an iterative inversion based on a fit of derived surface reflectance to a parameterised model (land or ocean), Rmod.

The SU v1.0 algorithm encompasses two distinct modules dedicated to separate surfaces: water & ocean on the one hand, land continental on the other hand.

6.1.1 Ocean surface model & aerosol retrieval

The module over water & ocean surfaces relies on AOD retrieval using channels from SLSTR S2 (670 nm) to SLSTR S6 (2.25 µm) & external surface reflectance estimation. The SLSTR S4 (1.37 µm – cirrus band) is excluded. This module assumes that the ocean surface Bidirectional Reflectance Distribution Function (BRDF) cannot be independently retrieved and/or decoupled from aerosol signals from SLSTR measurements. Therefore, it is exclusively estimated by including contributions from the glint reflectance (Cox and Munk, 1954) model, foam fraction & spectral reflectance (Monahan O'Muircheartaigh, 1980; Koepke (1984), and the Case I water reflectance (Morel, 1998) with a constant ocean pigment concentration of 0.1 mg/m^{-3}. The model is run coupled with the 6SV atmospheric Radiative Transfer Model (RTM) to account for sky glint. Corresponding values of ocean surface BRDF for a range of conditions are precomputed and stored in a Look-Up-Table (LUT) generated by the SU team. This LUT takes into account the geometry, wind, as well as the aerosol model and AOD for the contributions from atmospheric multiple scattering. The ocean surface is computed model at each wavelength as follows:

$$R_{Ocean} = w_{wc} * R_{wc} + (1 - w_{wc}) * (R_{glint} + R_{Chl})$$

With:

- R_{Ocean}, the total ocean surface reflectance
- R_{glint}, the glint reflectance
- R_{Chl}, the under-water light scattering due to chlorophyll
- R_{wc}, the white caps spectral reflectance
- w_{wc} , the fraction of ocean surface covered by white-caps.

The following is worth being noticed for the over ocean aerosol retrieval:

- The oblique view is used when available either as a second independent observation, or as the only observation constraining the retrieval if the nadir view is missing (*e.g.* due to sun-glint).
- The wind effects are corrected for *via* the ocean surface reflectance estimation per individual L2 AOD pixel. This is achieved by considering the wind speed and wind direction from the ECMWF forecast (available directly within the SLSTR L1B NRT product) and interpolated within the ocean BRDF LUT.
- The S1 channel (550 nm) is not used, to avoid potential large uncertainties caused by the ocean colour spatio-temporal variability.
- For glint an additional test is to be introduced based on the experience in of algorithm development during the ESA Aerosol CCI project. This additional test makes use of the tabulated values of ocean BRDF used for the ocean part of the aerosol retrieval. The LUT is used to estimate the ocean BRF in the 1.61 µm band for the viewing geometry of a given pixel assuming no AOD and a wind speed of 9m/s. Should the modelled ocean BRF exceed a reflectance of a threshold value of 0.008 the pixel is regarded as potentially glint contaminated and declared invalid.

6.1.2 Land surface model & aerosol retrieval

The module over continental land surfaces relies on all the 5 spectral channels from 550 nm to 2.25 µm & a joint aerosol-surface retrieval. It thus assumes that land surface BRDF & aerosol signals can be decoupled & simultaneously retrieved at all the wavelengths from the dual-view SLSTR acquisition. The sophisticated and physical multi-angular model defining the spectral change over land due to atmospheric scattering on the surface anisotropy, and thus the angular shape *i.e.* Bidirectional Reflectance Distribution Function (BRDF) as seen in the dual-view, spectral variation owing to the variation of the diffuse fraction of light, as a function of viewing angle (North *et al.*, 1999).The land surface reflectance computation is simplified by separating:

- a structural parameter P(Ω) representing the aggregate single scattering phase function that is only dependent on view direction Ω (*i.e.* anisotropy wavelength-invariant),
- from a spectral term ω(λ) corresponding to a Lambertian scattering albedo (*cf.* land surface colour) that is dependent only on wavelength λ (*i.e.* isotropy geometry-invariant).

Thus, these two parameters are assumed to be decorrelated. The model calculates the Top Of the Atmosphere (TOA) land surface reflectance as the linear sum of an anisotropic single scattered component and an isotropic multiply scattered component:

$$\rho_{land}(\Omega,\lambda) = (1 - D(\lambda))P(\Omega)\omega(\lambda)) + \frac{\gamma\omega(\lambda)}{1-g}(D(\lambda) + g(1 - D(\lambda)))$$

where $D(\lambda)$ is the diffuse fraction of light, γ is the fraction contributing to higher-order scattering, fixed at 0.3, and $g = 1 - \gamma\omega(\lambda)$.
It assumes that both $P(\Omega)$ and ω(λ) can be freely separated and the information content in the measurement is high enough to retrieve them independently.
The principal advantage of this model is that no *a priori* information of the land surface is required and aerosol properties can be retrieved over dark targets as well as bright areas. However, it does not make use of explicit additional spectral information assumptions related to the variable surface cover type. Such assumptions are typically crucial for aerosol retrievals from single view instruments which do not sample the angular domain.
The success of the aerosol inversion based on the multi-angular method in North *et al.* (1999) requires the following elements:

a) A minimum of two view angles and two wavelengths to solve independently the unknown parameters: P(Ω) and ω(λ).
b) A high enough aerosol measured signal and/or low enough surface model uncertainty to minimise AOD retrieval uncertainty.
c) The validity of the assumption of the wavelength-dependence of the atmospheric scattering layer anisotropy.

6.2 Additional elements

A lot of the original elements of the SU prototype v1.0 (see Sect.) were overall maintained in the current OSSAR-CS3 processor version of today (v3.0). These are notably:

- The approximation of the atmospheric Radiative Transfer (RT).

- The aerosol model Look-Up-Table (LUT).
- The a priori aerosol composition climatology.
- LUT approximation of RT coefficients.
- The numerical optimization scheme.
- AOD uncertainty computation.
- The aerosol models.
- *A posteriori* AOD uncertainty estimation.
- The assumed surface models & L1B prior uncertainty.

Further details on each of these elements are available in the Appendix A.

7 ALGORITHM EVOLUTION BASELINE TRANSFERRED INTO OSSAR-CS3

7.1 Overall motivation

EUMETSAT has performed a series of developments to enhance the algorithm quality as given in the precursor IPF v1. These developments are overall effective in OSSAR-CS3 since its 1st deployment as IPF v2.0 – Processing Baseline 1.0, in August 2020. They are motivated by the needs:

1) To work with the best radiometric calibration quality of the radiance: if, for any reasons, the quality requirements are not met in the available NRT L1B products, dedicated corrections are then explicitly applied to the radiances at the beginning of the L2 processor.
2) To include more explicitly the variability of the actual information content as a function geometry & surface type for an efficient aerosol-surface decoupling within SSAR as discussed in Sect. 5.3.
3) Prior to the L2 aerosol processing, to enhance the filtering of obstruction severely perturbing aerosol signal: this notably includes undesirable surface contamination, *e.g.* sediments in coastal waters, inland water, etc…, as well as opaque clouds, especially fractional layers over warm land surfaces.
4) Posterior to the L2 aerosol processing, to enhance the scientific quality flagging & identification of low retrieval performance based on physics indicators.
5) To minimize "system noise" in order to increase the capability of disentangling smooth (aerosol) from heterogeneous (surface) signals. This notably includes radiometric noise at high pixel resolution, potential dual-view mis-registration, nadir / oblique parallax residue, aliasing, etc....

Consequently, EUMETSAT has implemented the following components (see next sub-sections for further details):

- A global update of the SLSTR absolute, inter-band & dual-view calibration based on multiplicative gains obtained from vicarious calibration over desert sites and the consensus reached by 4 institutes (RAL, Rayference, CNES, Arizona University), verified & supported by the Sentinel-3 Validation Team (S3VT) atmosphere sub-group in December 2020 *via* research L2 aerosol algorithms, and eventually approved by EUMETSAT, ESA and the SLSTR Quality Working group (QWG). These gains are applied for L1B pixel measurements, and if no L1B quality indicator prevents the use of the associated radiance values.
- A set of optimized constraints applied to the SU Land model within the optimization scheme by combining 1) the inclusion of a 1st guess of the land surface reflectance in the visible, 2) weighted *a priori* constraints parameterized as a function of the dual-view geometry and the AFRI (see Sect. 5.3) for the land cover type identification, and 3) weights on spectral channels.
- Retrieval of log(AOD) instead of AOD to better cope with the non-linearity problem and slightly reduce computing time.

7.1.1 SLSTR spectral radiometry correction

As explained in the latest version of the L1B Product notice (PN) Sentinel-3 Product Notice – Level 1B: SL_1_RBT at NRT and NTC - S3.PN-SLSTR-L1.08 | EUMETSAT, the SLSTR solar channels (S1-S6) are known to have low to significant radiometric calibration issues.

More specifically, the SWIR bands (S5-S6) are non-compliant w.r.t. the mission requirements leading not only to highly inaccurate radiances in the SWIR but also non-consistent spectral signatures across the full Solar spectrum. Consequently, all solar channels have been undergoing a vicarious calibration assessment to quantify their radiometric calibration adjustment. Recent analysis of vicarious calibration results over desert sites performed by RAL, CNES, Rayference and University of Arizona have determined new and consistent radiometric deviations w.r.t. common reference sensors (MERIS, MODIS) [S3MPC.RAL.TN.010]. These have been used to provide a first-order radiometric corrections with more detail available in [S3MPC.RAL.TN.020].

Given the typical order of magnitude of the aerosol signal aimed at being fitted (see Figure 6), it is essential to ensure the upmost L1B radiance quality at the beginning of the L2 processing. Current radiances in the SLSTR L1B product remain uncorrected of these radiometric calibration adjustments. Hence, all multiplicative coefficients listed in Table 2 are applied to update the SLSTR absolute, inter-band & dual-view calibration. These coefficients are similar for both SLSTR S3A & S3B, for all L1B radiances at fine pixel resolution (500 m), and before any further L2 processing (*i.e.* cloud filtering, super-pixel aggregation, etc…). The corrections were calculated for S3A but are equally applicable to S3B because S3B has been harmonised to S3A during the commissioning phase [RD-5]. Residual differences (<1%) between S3A and S3B after harmonisation are yet observable, but not accounted for at this stage in OSSAR-CS3.

SLSTR Views	S1	S2	S3	S5	S6
Nadir	0.97	0.98	0.98	1.11	1.13
Oblique	0.94	0.95	0.95	1.04	1.07

Table 2: Multiplicative coefficients in the OSSAR-CS3 processor to update of the SLSTR absolute, inter-band & dual-view calibration, for each individual L1B pixel at fine resolution, prior any further L2 processing [S3MPC.RAL.TN.010] Sentinel-3 Product Notice – Level 1B: SL_1_RBT at NRT and NTC - S3.PN-SLSTR-L1.08 | EUMETSAT

The following is emphasized:

- Uncertainties associated with each of these coefficients are not yet used today.
- All coefficients are applied, even if the magnitude is lower than the estimated uncertainty. The main reason is to ensure the best inter-band recalibration while the optimization scheme fits both AOD, and the aerosol model, requiring then the most accurate reflectance spectral shape.

Many benefits have overall been observed since these coefficients are applied. Notably:

- Over ocean background, AOD(550 nm) values are either increased or decreased depending on the geometry & meteorology conditions. Generally, a bias present with IPF v1.0 is reduced in the IPF v2.0, with a strange North-South feature being removed (internal analyses & informal communication from CAMS).
- AOD(550 nm) values associated with a high (Saharan) dust load over the Atlantic ocean are strongly reduced. Theoretical studies based on SARP simulations confirm that the SWIR mis-calibration, and the negative spectral gradient artefact w.r.t. the visible channels, is the root cause of a significant positive bias (up to 0.2) due to the selection

of a too high scattering aerosol model during the optimization (see Figure 10 [RD-2]). Furthermore, match-up with L2 AOD pixels from NASA MODIS Terra, Collection 6.1 – Dark target (DT) Ocean, with the outputs from the IPF v1.0 used to show a high gap for high dust AOD of the same magnitude (see Figure 11). Such large positive differences were considered as abnormal as, in such situations, MODIS AOD DT Ocean is known to have a potential bias due to the use of spherical instead of spheroid model, more adequate w.r.t. dust particle shape (Zhao *et al.*, 2003; Lee *et al.*, 2017; Zhou *et al.*, 2020).

- Estimation of the 1st guess of the land surface reflectance requires overall a highly accurate spectral & inter-band calibration quality (see Sect. 7.1.2).

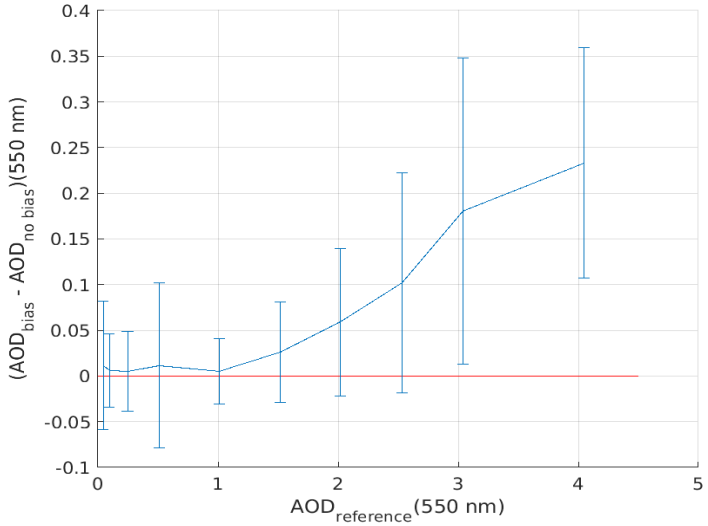

Figure 10: Theoretical AOD(550 nm) retrieval error over ocean surfaces caused by negative bias on the SLSTR SWIR radiance of -10%. AOD reference (550 nm) is the true AOD value considered in the simulation, while the AOD(550 nm) error is on the y axis. Extracted from the EUMETSAT state funded SARP study, performed by FMI (cf. [RD-2]).

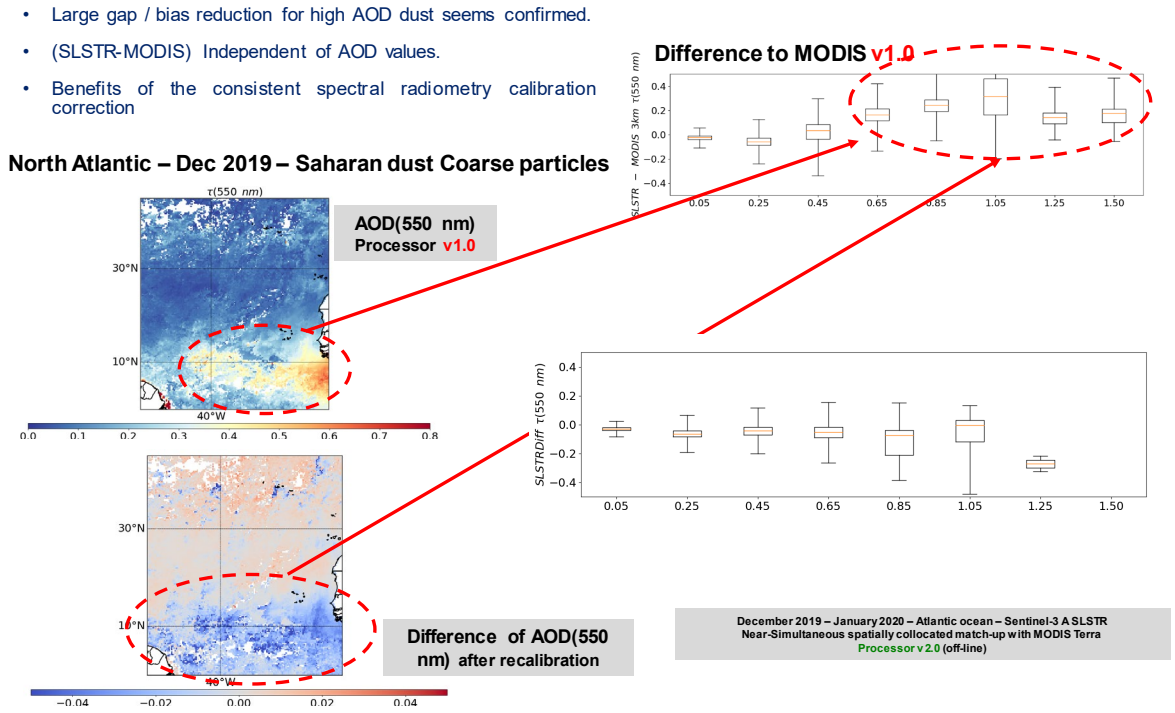

Figure 11: Benefits of the update of the SLSTR absolute, inter-band & dual-view calibration on the AOD(550 nm) retrievals associated with high dust load over ocean surfaces. A too large positive departure was observed with the precursor IPF v1.0, spatially collocated with MODIS terra Collection 6.1. Since IPF v2.0, this departure is largely reduced.

7.1.2 Estimating spectral Land Surface Reflectance (LSR) 1st guess: the AFRI Red-SWIR LSR

The analyses of Sect. 5.3 indicate the lack of sufficient information content provided by dual-view sensors for allowing a completely independent application of the SSAR concept on an operational global & daily basis. Preliminary analyses suggest this is mostly critical over vegetation land covers, from medium to high vegetation bloom. This is true, regardless of the dual-view orientation, and is primarily related to the too limited number of views.

To address this challenge, the following idea has been developed: since, the key goal is first the retrieval of aerosol properties, and there is not enough always enough information in the dual-view measurements to retrieve without constraints both aerosol & land vegetation surface properties independently, an independent first guess on the land vegetation surface reflectance is hence required. This 1st guess goal is primary to increase the constraint on the land vegetation surface reflectance such that the ambiguity between aerosol & surface signals is minimized and the associated decoupling is more performant for a good AOD retrieval quality.

At the moment of writing, there is no suitable external auxiliary dataset to consider as a 1st guess for SLSTR. Therefore, first guess land vegetation surface reflectance in the red band (SLSTR S2 – 0.6 µm) is independently estimated, on the fly per individual AOD L2 pixel. It exclusively relies on a spectral methodology & using the AFRI index estimated from SLSTR measurements corrected of gas absorption & Rayleigh scattering (see Sect. 5.3).

AFRI presents the following advantages:

- Firstly, AFRI & NDVI (from surface reflectance) present a very high correlation. This is mostly true for high vegetation covers, which is the 1st high priority here. Some dispersion for complex hybrid & urban soils reveals a lower vegetation over lands with lower vegetation density, This is howver acceptable at this stage as these surfaces have lower priorities for this 1st guess. For both indexes, low / high values correspond to bare / high vegetation density surface covers respectively (see Figure 12 & Figure 13). This high correlation between AFRI & NDVI is explained by the fact that land surface reflectance in the SWIR (2.25 µm) channel, used in AFRI, highly correlates with the red band (0.6 µm), used in NDVI (see Figure 16).
- Secondly, for most of low and medium atmospheric aerosol load cases, AFRI is little impacted by the aerosol signal & associated surface pattern does not present interferences by widely spread fine particle plumes (see Figure 14 & Figure 15). Therefore, in many cases, it is not only possible to directly estimate it from SLSTR measurements per AOD pixel, but also use it in subsequent steps. This is mostly thanks to the little impact of fine particles in the long-wavelengths. Exceptions are likely 1) in case of dust particles, which may display a high signal in the SWIR, and 2) very high AOD(550 nm) values (larger than 1 – see Figure 15). However, the impacts of high AODs is mostly over lands with low vegetation density. These limitations will be addressed in a next evolution of OSSAR-CS3.

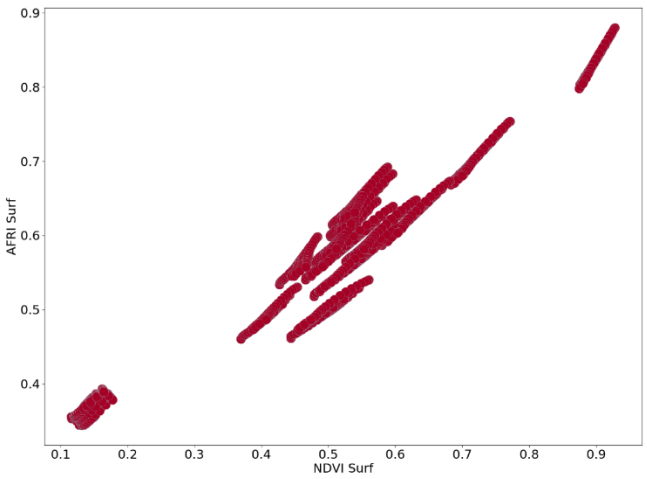

Figure 12: Relationship between the AFRI & NDVI vegetation indexes, both computed from surface reflectance. Based on the simulated database produced within the SARP project [RD-2].

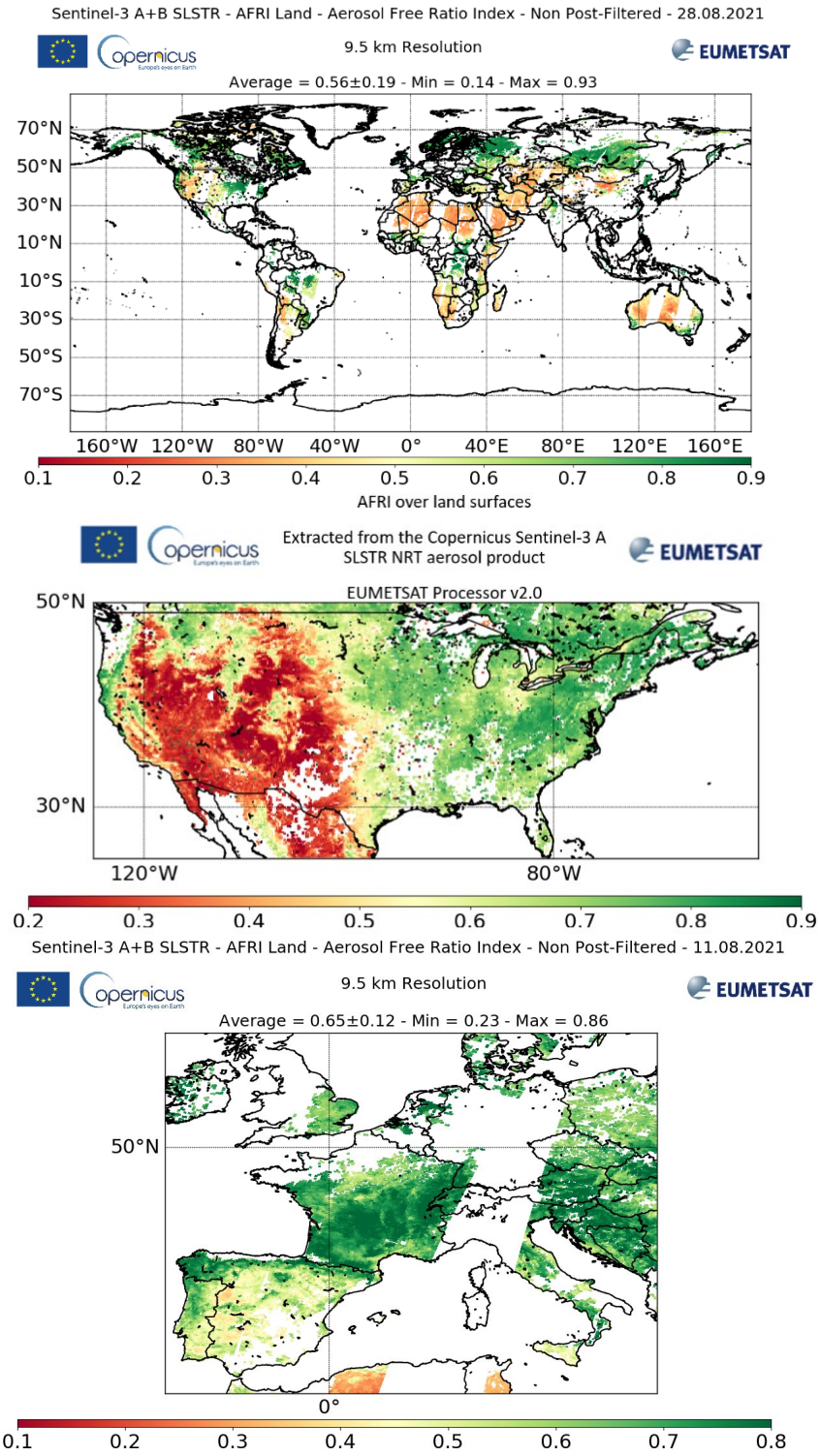

Figure 13: Mapping of the AFRI land cover index, estimated from the SLSTR S3 & S6 measurements. High values represent high vegetation density while the lowest values are associated with bare soils. Intermediary values (around 0.5) correspond to hybrid / urban soils with a mixture of low to medium vegetation density & bare soils. Top: daily map from S3A+S3B on 28.08.2021; Middle: Monthly average from S3A (Winter); Bottom: 1 day in Summer 2021 over Western Europe (high vegetation in France & Germany, drought conditions in Spain & Italy, bare soils in Northern Africa).

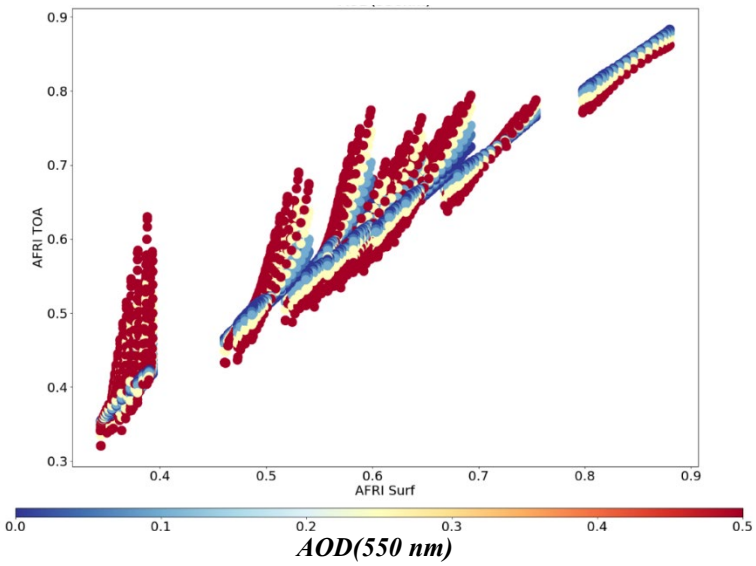

Figure 14: Relationship between AFRI TOA (*i.e.* AFRI computed from TOA reflectance) and AFRI Surface (*i.e.* AFRI computed from surface reflectance) as a function of AOD(550 nm).

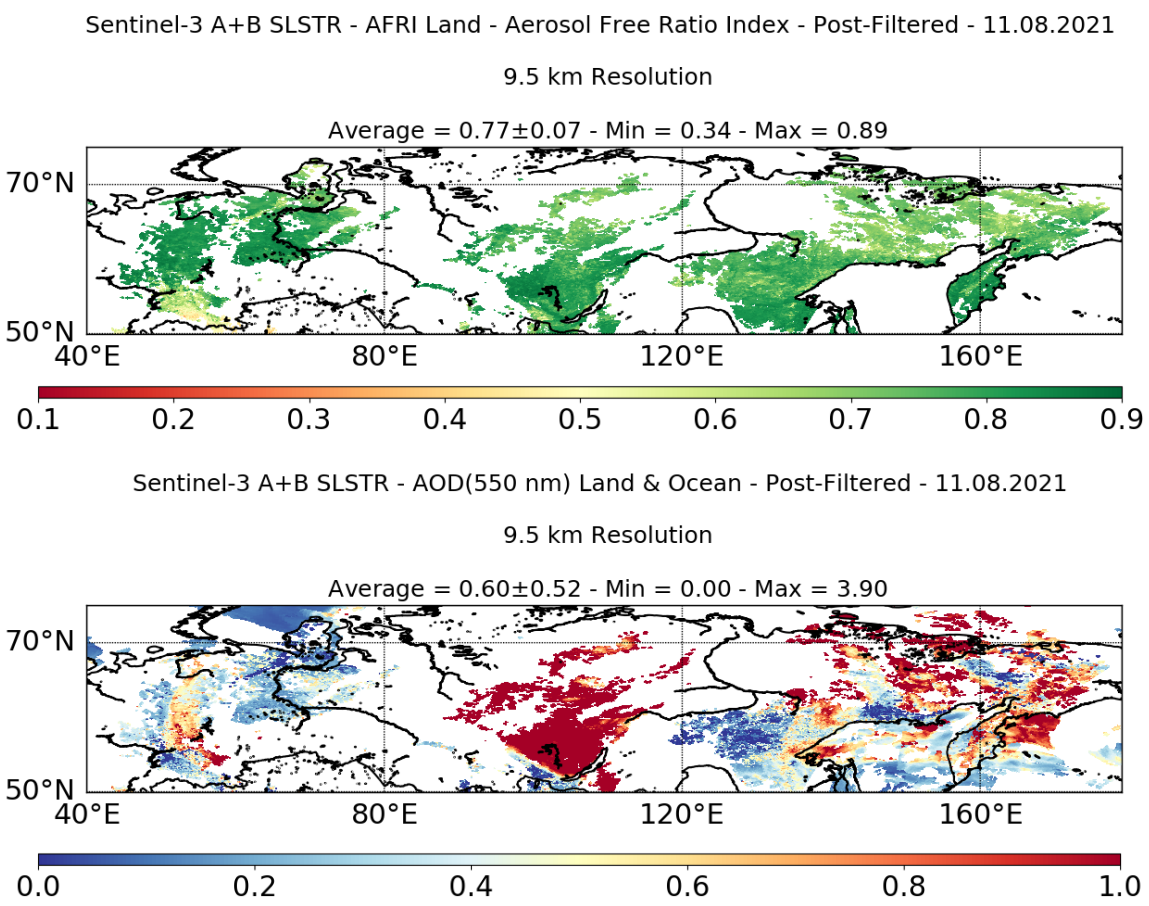

Figure 15: S3A+S3B SLSTR – AFRI & AOD(550 nm) from PB 2.0 – IPF v3.0.

The 1st guess estimation methodology builds upon the strong correlation of the surface reflectance in the red (SLSTR S2) and the NIR (S3) and SWIR (S6) bands and their connection w.r.t. land cover types identified thanks to AFRI (see Figure 16 & Figure 17). For each AOD

super-pixel (9.5 km), and each view (nadir & oblique), the far SWIR (S6 detector – 2.25 µm) & NIR (S3 detector – 0.8 µm) spectral reflectances are corrected of atmospheric gas transmission & Rayleigh scattering: $RLand_{S6}$ & $RLand_{S3}$ respectively.

Secondly, AFRI is estimated per each AOD super-pixel (9.5 km) & for each view (nadir & oblique).

Thirdly, the land surface reflectance first guess in the red band is estimated depending on the AFRI:

- For medium to high developed vegetation, *i.e.* AFRI in the range of [0.75:0.9]:

$$RLand_{S2} = a(AFRI) * RLand_{S6}$$

- For low to medium vegetation, *i.e.* AFRI in the range of [0.55:0.75]:

$$RLand_{S2} = a(AFRI) * RLand_{S3}$$

With:

- $RLand_{S2}$, the estimated land surface reflectance in the red (SLSTR S2 – 0.6).
- $a(AFRI)$, a simple multiplicative coefficient empirically derived from the SLSTR spectral synthetic database generated within the frame of the EUMETSAT SARP project https://www.eumetsat.int/SARP. $a(AFRI)$ is estimated for every AFRI sampled with a regular interval of 0.05.

The switch from $RLand_{S6}$ to $RLand_{S3}$ is motivated by the fact that, over hybrid / urban soils with low vegetation density, the surface reflectance correlation between the SWIR & red bands is quite decreased while it remains still very high between the NIR and red (see Figure 16 & Figure 17). Similar findings are noted by Hsu *et al.*, 2019. Overall, it shall be emphasized how critical is the SLSTR inter-band calibration quality (see Sect. 7.1.1) in order to ensure a reliable 1st guess estimation.
Finally, this 1st guess is included in the optimization scheme (see Sect. 7.1.5). Given the higher diversity of the values & the non-obvious correlation with any of the other reflectance in the long wavelengths, the land surface reflectance 1st guess in the green band (SLSTR S1 -) is not estimated, leading then to a reduction of the use of this channel.

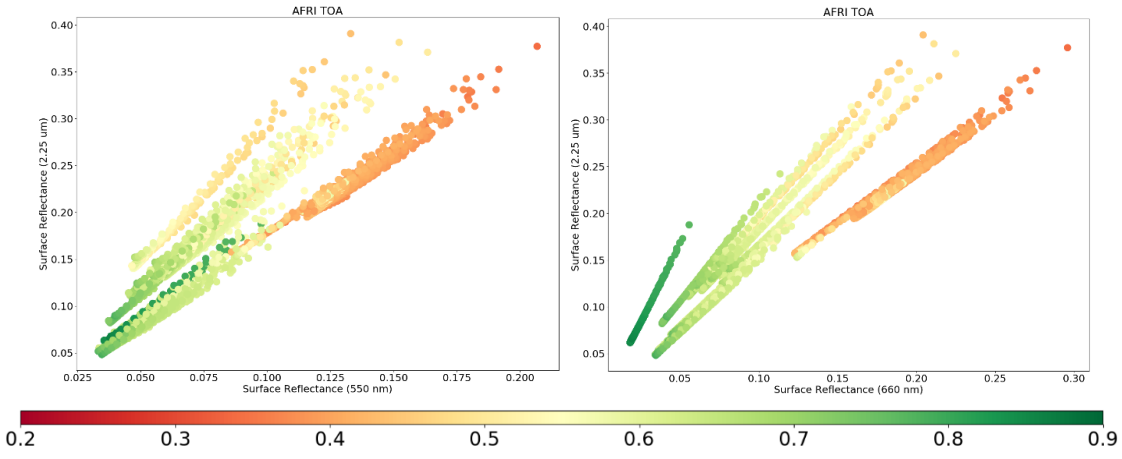

Figure 16: Relationship between surface reflectance at different SLSTR wavelengths as a function of AFRI. Left: 2.25 µm *vs.* 550 nm; Right: 2.25 µm *vs.* 660 nm.

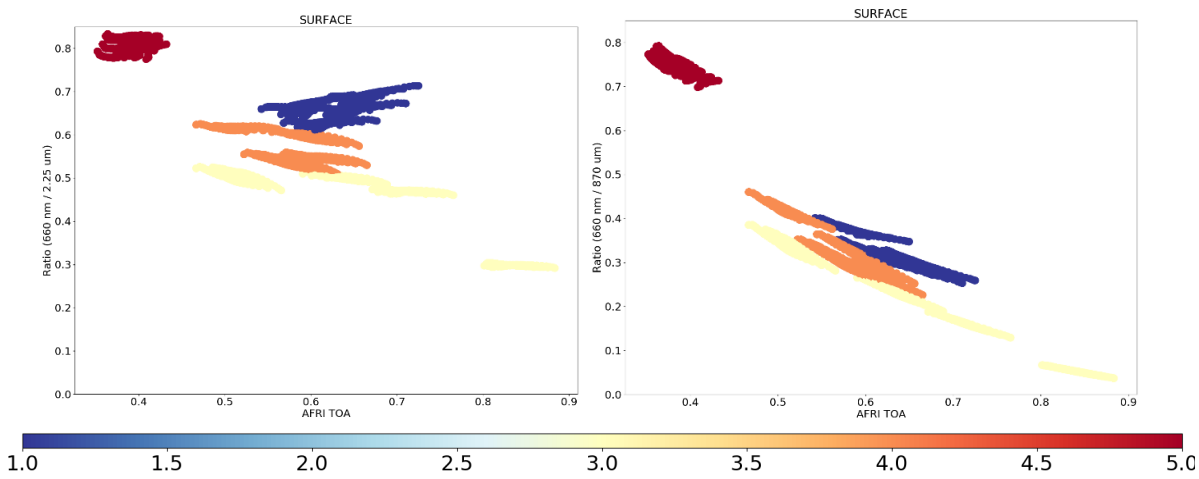

Figure 17: Relationship between ratio of surface reflectance at different SLSTR wavelengths as a function of AFRI. Left: S2/S6; Right: S2/S3.

7.1.3 Optical Cloud Mask – Land

7.1.3.1 Rationale

Cloud filtering is a critical pre-requisite before any attempt of aerosol retrieval. Cloud residuals, *i.e.* not screened, will generally lead to abnormal AOD values (very often too high) and potentially a too high spatial heterogeneity in the retrieved aerosol plume. While most of these outliers could be expected to be identified & removed *via* the *a posteriori* quality filtering (see Sect. 7.1.9), a non-negligible number may be missed & conserved in the final product. Indeed, ambiguity is sometimes possible between aerosols and small broken clouds left in the L2 super-pixel and/or thin cirrus which may present similar signals.

The currently used basic cloud mask from the SLSTR L1B product (see Sect. 4.2) is not developed w.r.t. aerosol requirements. At the time of the precursor IPF v1.0 development (see Sect. 5.1), there was no other cloud mask opportunities to be imported. Various analyses until now overall reveal a significant inadequacy between the L1B basic cloud mask & the scientific needs for operational L2 aerosol processing. Especially, a large percentage of clouds are overall under-screened over land surfaces leading to a too high number of residuals in the retrieved AOD. Internal analyses and exchanges with the Copernicus S3MPC reveal that the root cause is an under-exploitation of the SLSTR Solar channels over land surfaces which especially miss i) clouds over bright soils (desert, urban, hybrid, crops), and ii) fractional small clouds over warm vegetation. Most of them lack a strong thermal contrast between their top layer & the surface underneath making the TIR cloud tests insufficient for cloud filtering.

The priority, at the moment of the Collection 2 preparation, is to implement within OSSAR-CS3 an optical cloud mask over land surfaces prior to aerosol retrieval & only use the TIR cloud tests coming from the L1B basic cloud mask. Note that the few visible cloud tests from the L1B are not considered anymore.

The prototyping of the optical cloud mask over lands relies on the following experiences:

- All success cloud tests applied on the NASA MODIS, NOAA VIIRS & ABI, and Metop (*cf.* PMAp) sensors for supporting operational aerosol applications.

- Extensive literature review & experiences acquired *via* the EUMETSAT Member state funded activity named "Sentinel-3 SYNergy Cloud Mask (S3 SYN CM)", in progress at the time of the writing of this ATBD https://www.eumetsat.int/S3-synergy-cloud-mask
- Planned cloud tests for the future EPS-SG METimage sensor.

All *a priori* land cloud tests described below are overall applied at the original fine L1B resolution, *i.e.* 500 m, in both SLSTR views. The key motivation is the *a priori* identification and removal of opaque layers with a high obstruction degree hampering the aerosol signal. These are overall complementary to the enhanced *a posteriori* filtering of AOD outliers including potential few residuals (see Sect. 7.1.9). Examples of the optical land cloud mask are illustrated in Figure 18 & Figure 19.

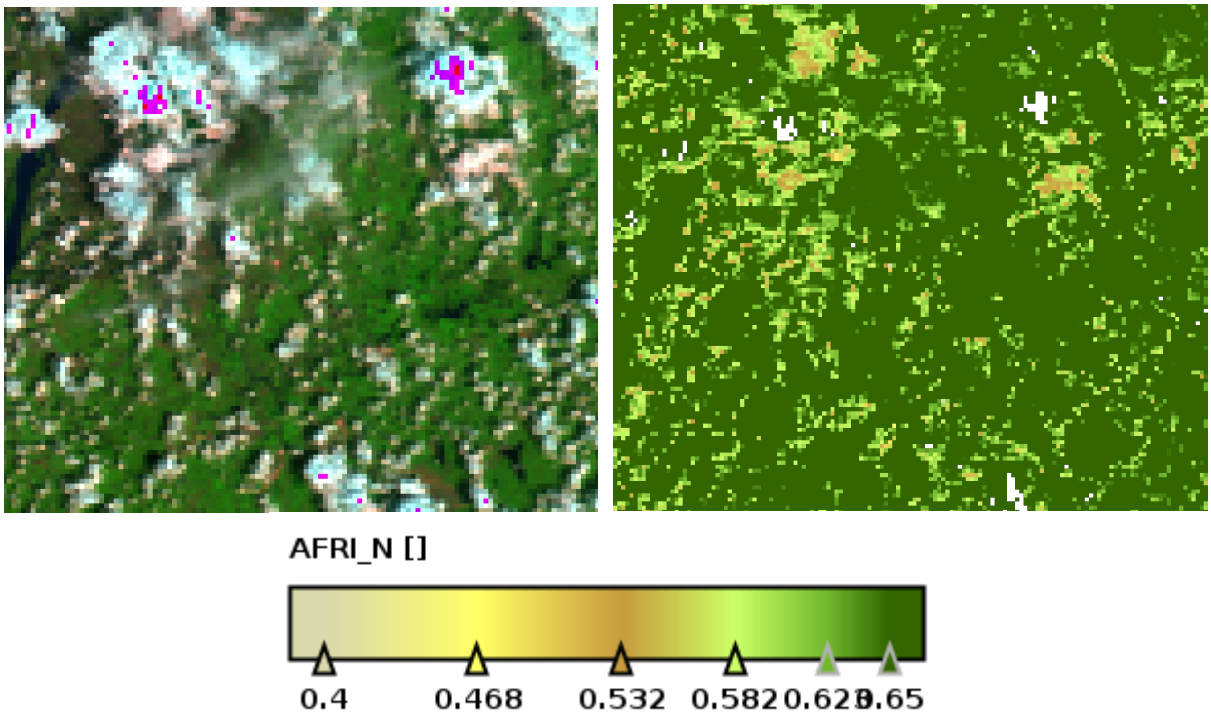

Figure 18: S3B SLSTR 2021.08.18 nadir view over East-China land (from S3B_SL_1_RBT____20210818T022301 NRT). Left: RGB; Right: AFRI.

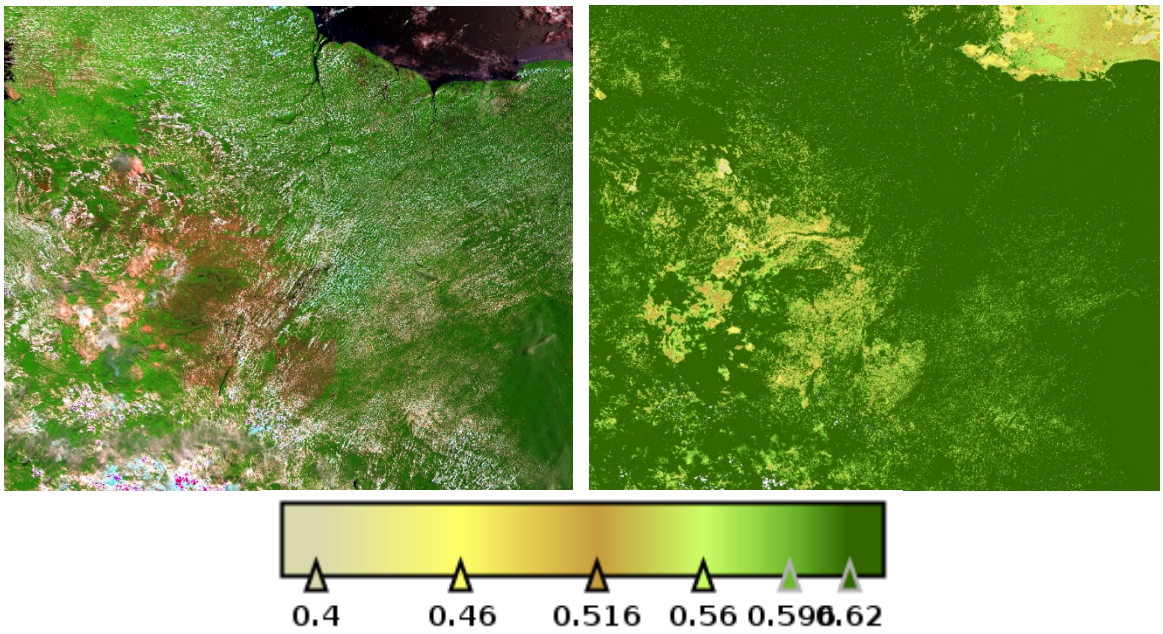

Figure 19: S3A SLSTR 2021.09.01 nadir view over South-America (from S3A_SL_1_RBT____20210901T135437NRT). Left: RGB; Right: AFRI. High number of small broken clouds over forest vegetation is visible in top and right parts of the image.

7.1.3.1.1 NIR / Red ratio test

Cloud spectral reflectance is known to be quite similar across the red S2 (0.65 µm) & NIR S3 (0.85 µm), while waters & high vegetation covers display a strong gradient. Hence, the SLSTR S3/S2 ratio can be expected to be lying in the range of [0.9:1.1] over clouds, while cloud-free well-developed vegetation surfaces usually show values much greater than 1 (Ackerman *et al.*, 2006). This ratio test cannot be applied over arid & semi-arid ecosytems, which display a broad range values which can be confused with clouds.

Therefore, the SLSTR NIR / Red ratio test is exclusively applied over high vegetation covers. A single SLSTR L1B pixel (500 m) is assigned as very opaque cloud if:

$$AFRI \geq 0.62$$
and
$$\frac{R_{S3}}{R_{S2}} \leq 1.35$$

These thresholds are applied on the sun-normalized radiances, and not reflectance (*i.e.* viewing zenith angles are not accounted for). They were identified based on internal analyses and training on reference cases.

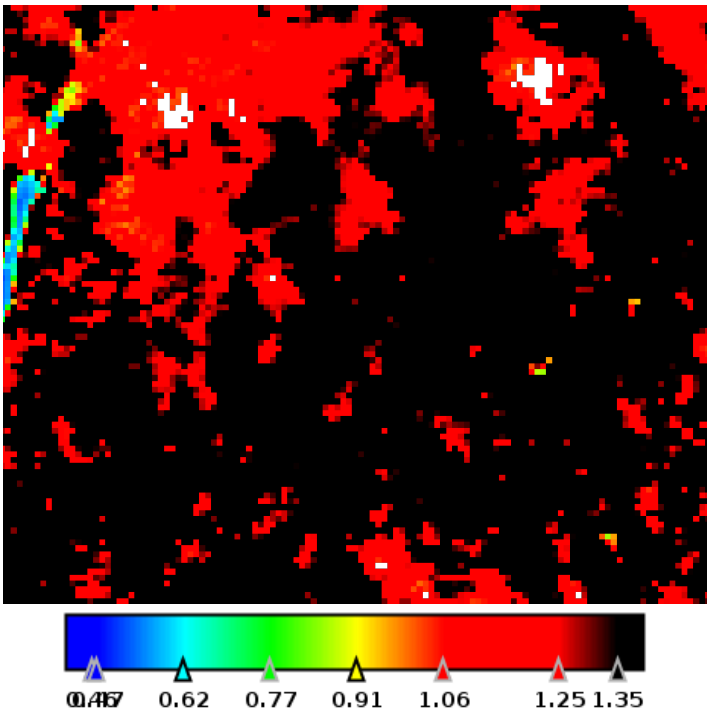

Figure 20: SLSTR ratio of S3/S2 sun-normalized radiances from nadir view from S3B SLSTR 2021.08.18 over East-China land (from S3B_SL_1_RBT____20210818T022301 NRT) – see Figure 18. Pixels not in black, combined with the AFRI threshold are identified as clouds.

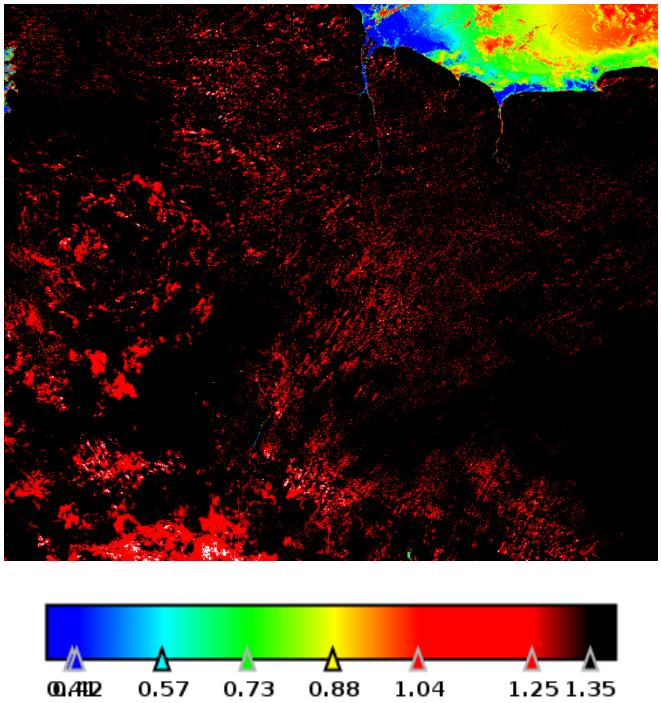

Figure 21: SLSTR S2 sun-normalized radiance from nadir view from S3A SLSTR 2021.09.01 nadir view over South-America (from S3A_SL_1_RBT____20210901T135437 NRT) – see Figure 19. Pixels not in black, combined with the AFRI threshold are identified as clouds.

7.1.3.1.2 Red absolute test

Over vegetated land, reflectance from the 0.65 µm (S2 band) can help to discriminate bright clouds from dark surfaces. While traditional thresholds are functions of background NDVI and scattering angle (Hutchison *et al.*, 2005), a default value is used here as inspired by the MODIS cloud mask (Ackerman *et al.*, 2006).

The SLSTR red absolute test is only applied over land covers presenting low to high vegetation bloom, including hybrid (*i.e.* mixture of vegetation with urban) soils. A single SLSTR L1B pixel (500 m) is assigned as very opaque cloud if:

$$AFRI \geq 0.55$$
and
$$R_{S2\geq}\ 0.12$$

These thresholds are applied on the sun-normalized radiances, and not reflectance (*i.e.* viewing zenith angles are not accounted for). They were identified based on internal analyses and training on reference cases. A balance was empirically found such that this absolute threshold on the S2 sun-normalized radiance is high enough to avoid filtering pixels with a high load of aerosol pollution, but unambiguous opaque clouds are screened.

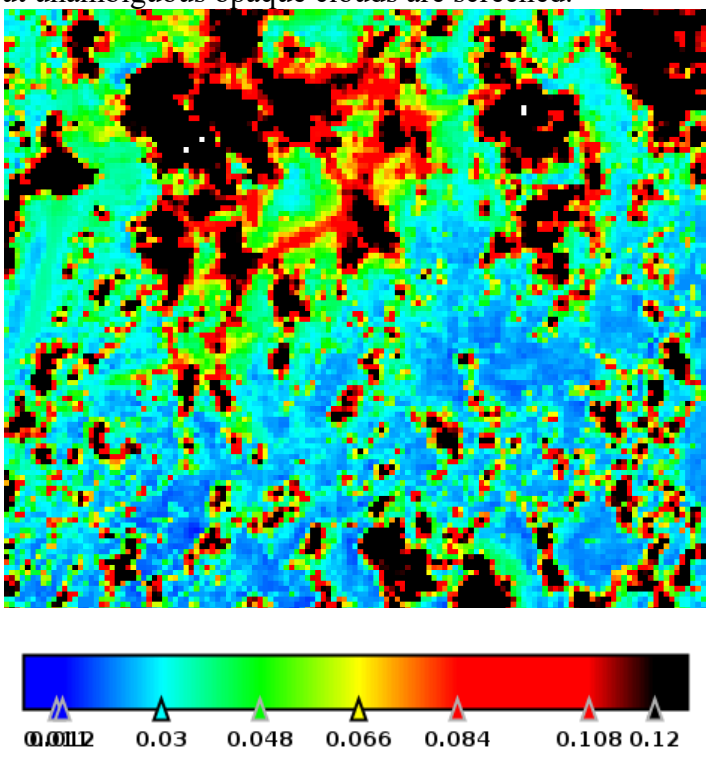

Figure 22: SLSTR S2 sun-normalized radiance from nadir view from S3A SLSTR 2021.09.01 nadir view over South-America (from S3A_SL_1_RBT____20210901T135437NRT NR) – see Figure 18. Red/black pixels, combined with the AFRI threshold, are labelled as clouds.

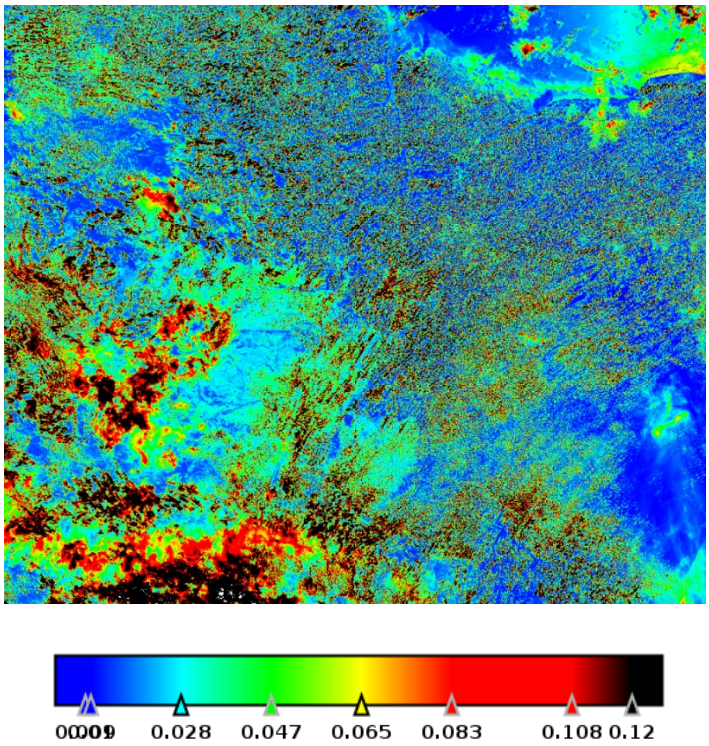

Figure 23: SLSTR S2 sun-normalized radiance from nadir view from S3A SLSTR 2021.09.01 nadir view over South-America (from S3A_SL_1_RBT____20210901T135437 NRT) – see Figure 19. Red/black pixels, combined with the AFRI threshold, are labelled as clouds.

7.1.3.1.3 Clear-Sky visible spatial uniformity

The presence of a small cloud shall increase the local spatial heterogeneity beyond the natural surface variability expected for a clear sky. As applied to many cloud imagery sensors such as ABI (Ackerman *et al.*, 2013), the spatial uniformity test based on the red (typically around 0.6 µm) is generally quite powerful for detecting low fractional clouds, even over bright surfaces. It generally needs 1) to be restricted to a very small area (over large areas, high surface heterogeneity is naturally expected), and 2) the availability of measurements at a high spatial resolution (lower than 1 km). Ambiguity with aerosol plumes should be expected as quite unlikely due to their generally homogeneous horizontal properties over wider distances.

Consequently, the SLSTR clear-sky visible spatial uniformity is only applied to SLTR L1B pixels (500 m) non flagged as clouds by the previous steps, and within a box area of 3 x 3 (*i.e.* < 1.5 km). If:

$$Std\ (R_{S2}) \geq 0.41 * Min(R_{S2})$$

With:

- $Std\ (R_{S2})$, the standard deviation of R_{S2} over the 3 x 3 box area
- $Min(R_{S2})$, the minimum of R_{S2} over the 3 x 3 box area.

The threshold of 0.41 is applied on the sun-normalized radiances, and not reflectance (*i.e.* viewing zenith angles are accounted for). It is inspired by the figure 26 of Ackerman *et al.* (2013), and internal training. The main difference at this stage is the consideration of the minimum SLSTR S2 reflectance within the 3x3 box instead of an assumed clear-sky

reflectance. However, it has to be noted that the combination of this specific test with the *a posteriori* quality filtering in Sect. 7.1.9, is actually quite similar to the planned cloud uniformity tests for MetImage on the EPS-SG satellite: a pixel will be labelled as cloudy if the standard deviation in the box centred at the pixel is higher that the clear –sky standard deviation, and if the difference between the pixel reflectance and its expected clear-sky reflectance is higher than the mean value found inside the box.

7.1.3.1.4 Enhanced brightness neighbouring – Cloud Margin

For each SLSTR L1B pixel (500 m) flagged as Cloud, either *a priori* by the SLSTR L1B cloud mask, or as very opaque by the optical land cloud tests above, a safety margin is built to account for 3D scattering effects at small scales that may lead to an enhanced signal measured over a clear-sky land cover. The basic assumption is that such a 3D effect can propagate over a distance of ~3km in each direction.

Consequently, every 6 x 6 L1B pixels located around a SLSTR L1B pixel (500 m) flagged as Cloud in the previous steps is labelled as cloud and is then rejected in the aggregation of the AOD super-pixel.

7.1.3.2 Illustrated benefits

The overall benefits can be seen in the next Figure 24, Figure 25, Figure 26, and Figure 27:

- In general, the SLSTR l1B basic cloud mask fails to identify all the small broken clouds over vegetation surfaces. This leads to a large amount of abnormally high AOD(550 nm) values in PB1.0, especially in the northern part of South-America. Even if a large fraction could be removed, the *a posteriori* filtering of PB 1.0 left a non-negligible amount of these AOD pixels in the final product. Retrieved smoke plumes over Siberia show overall very noisy patterns with PB 1.0 due to the mixture of real aerosol particles, with unscreened cloud residuals. Note also that the bias in the retrieved AOD due to lower quality in AOD land retrieval at that time.
- In the PB 2.0, not only most of cloud layers are now successfully *a priori* detected by land optical cloud mask, but also combined with the enhanced a posteriori filtering (see Sect. 7.1.9), and the final AOD values rarely show cloud residuals over vegetation covers. Siberian smokes show much smoother patterns, with similar structures to MODIS Terra – Merged DT/DB from NASA Collection 6.1.

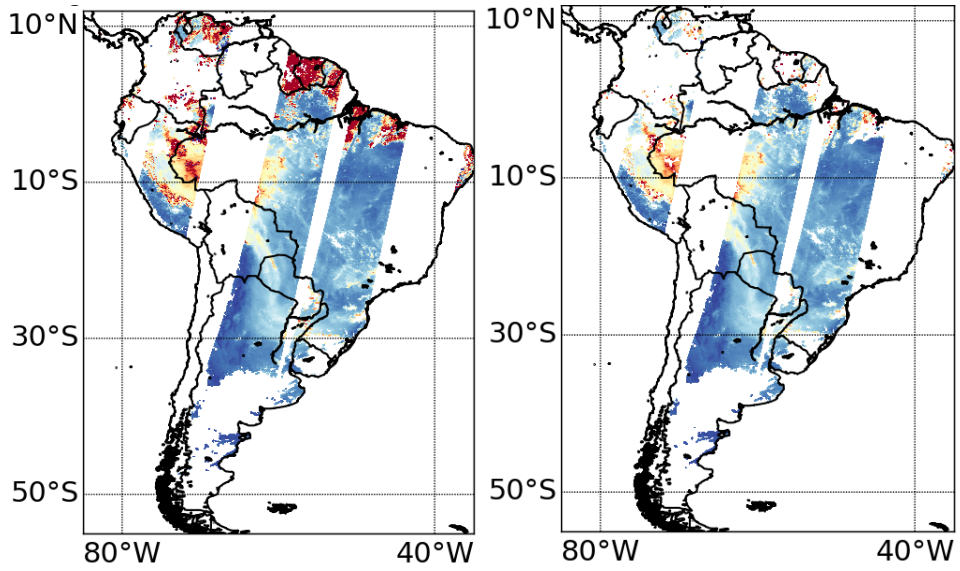

PB 1.0 – IPF v2.0

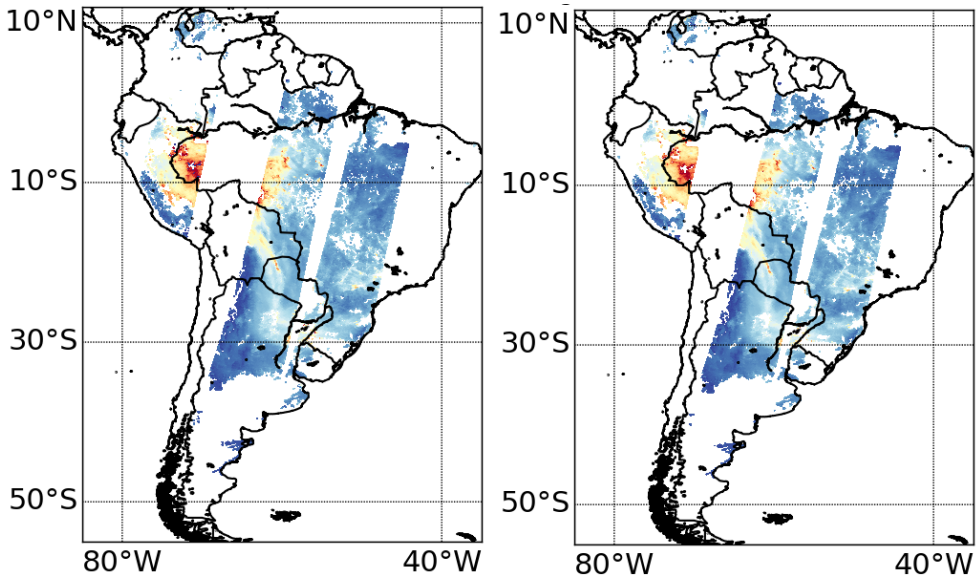

PB 2.0 – IPF v3.0

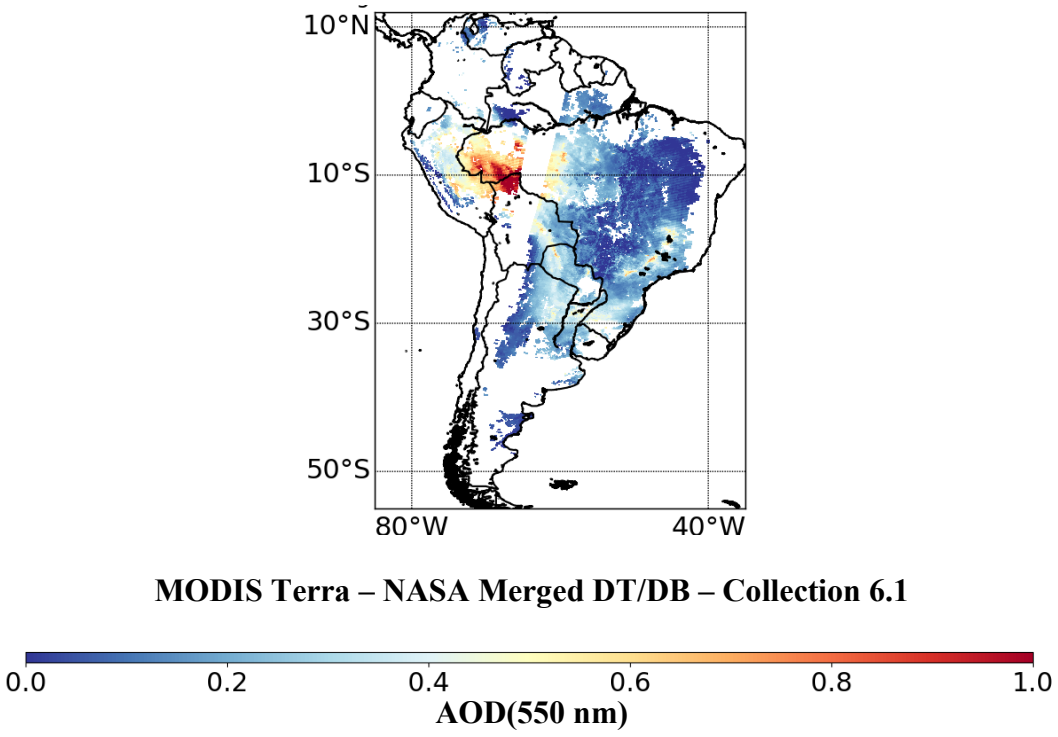

Figure 24: Impact of the new optical cloud mask – 17.08.2021, S3A + S3B – Fractional cloud issues over the Amazonian forest in South-America.

Top: PB 1.0 – IPF v2.0 (exclusively based on the SLSTR L1B basic loud mask for both land and oceans urfaces) – Left: AOD(550 nm) land all quality before *a posteriori* quality. Right = AOD(550 nm) land best quality, after *a posteriori* quality.

Bottom: PB 2.0 – IPF v3.0 (with the optical land cloud mask) - Left: AOD(550 nm) land all quality before a posteriori quality. Right = AOD(550 nm) land best quality, after a posteriori quality.

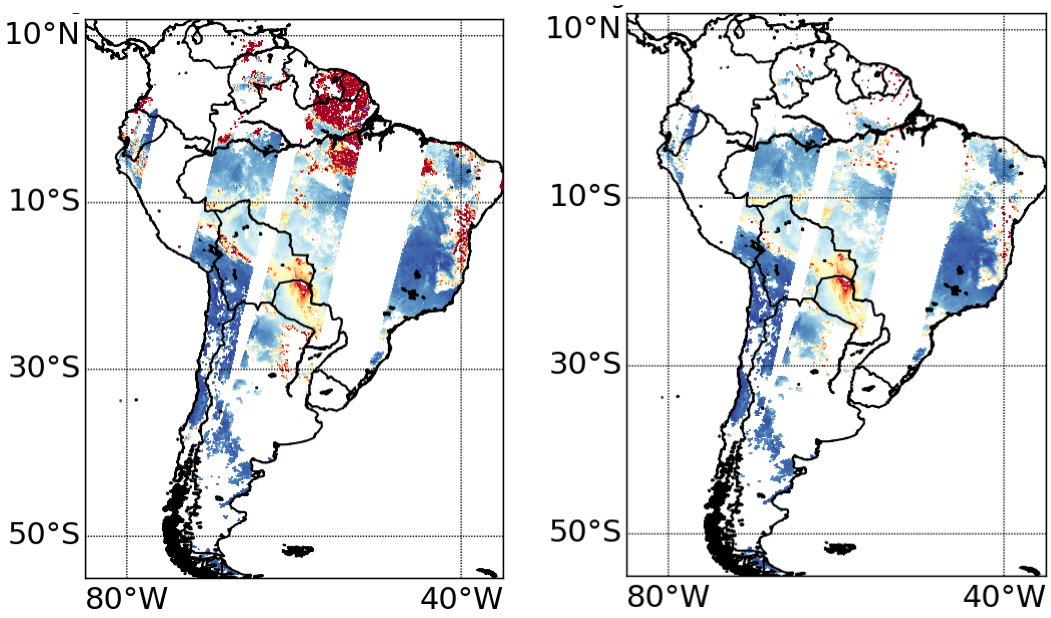

PB 1.0 – IPF v2.0

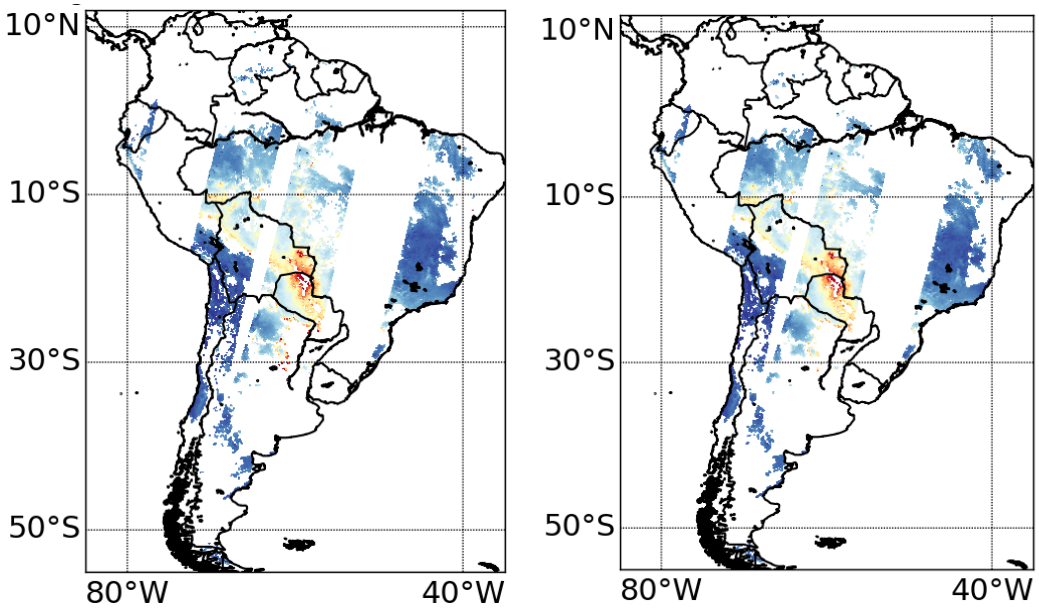

PB 2.0 – IPF v3.0

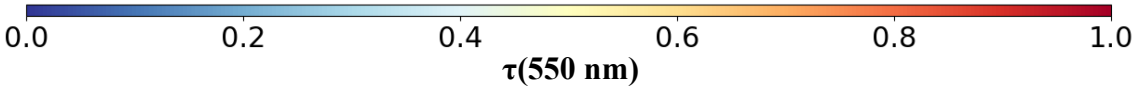

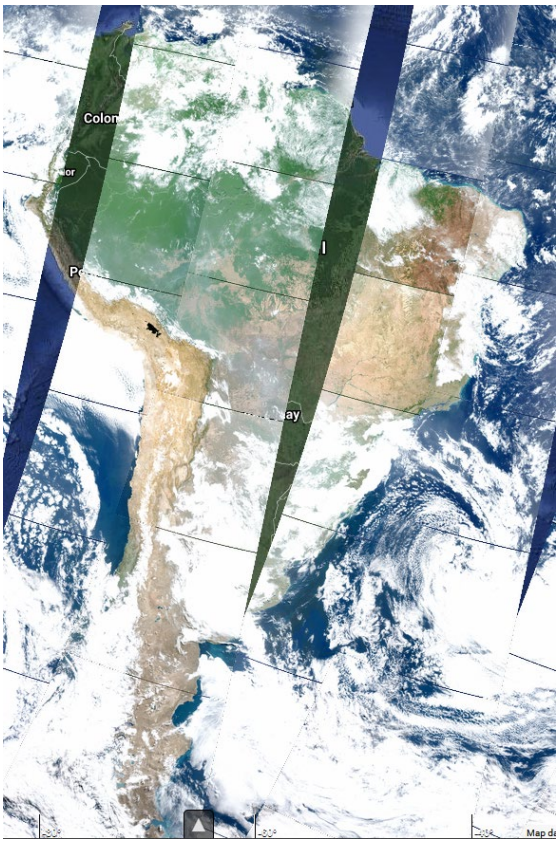

Figure 25: Same as Figure 24 – 04.09.2021, S3A + S3B – Fractional cloud issues over South-America.

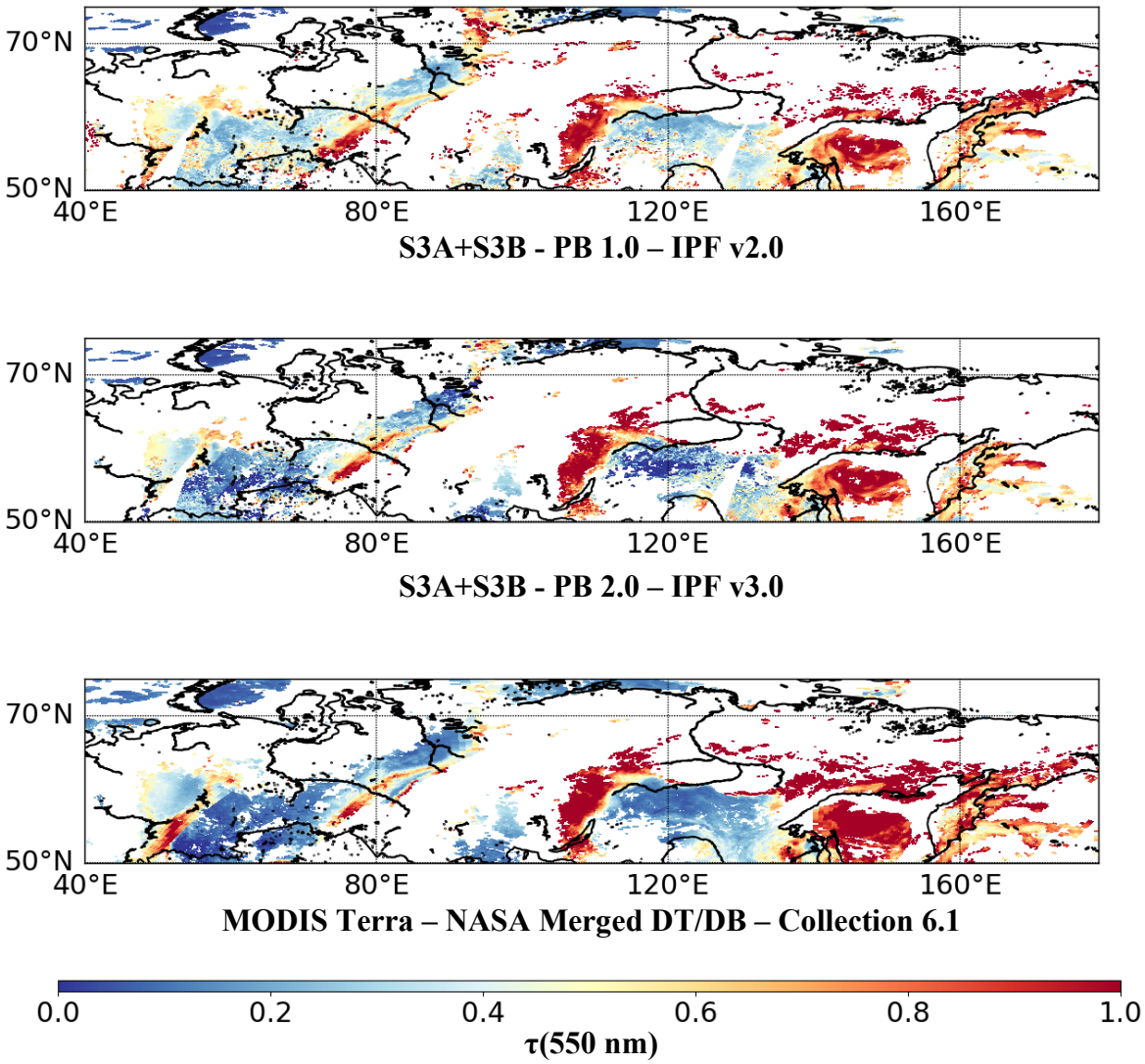

Figure 26: Impact of the new optical cloud mask + improvements brought by the AFRI Red-SWIR LSR model – 13.08.2021, Siberia wildfire – Fractional cloud issues & mixture with smoke.

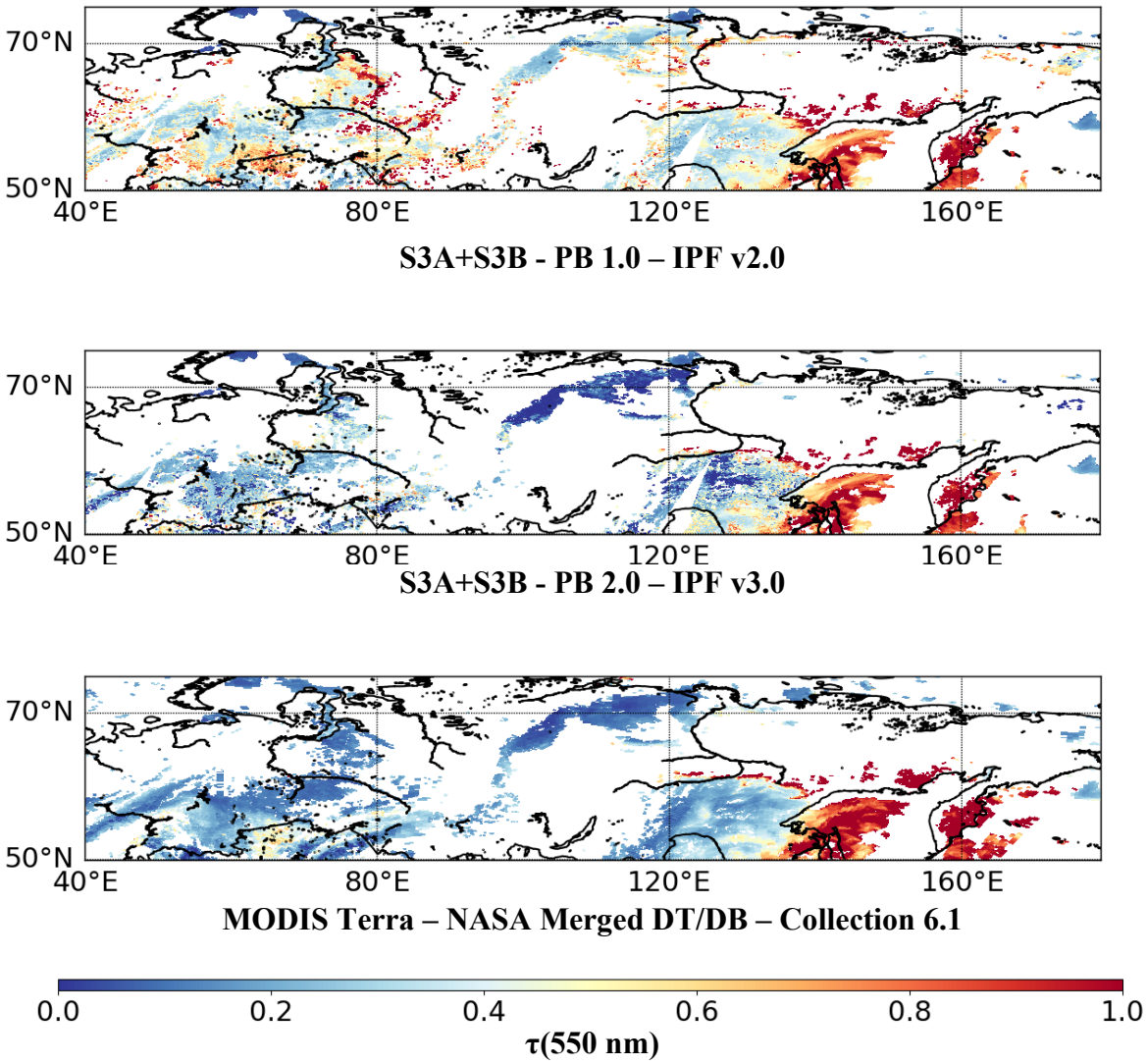

Figure 27: Impact of the new optical cloud mask + improvements brought by the AFRI Red-SWIR LSR model – 13.08.2021, Siberia wildfire – Fractional cloud issues & mixture with smoke.

7.1.4 Rejection of inland water contamination

The surface type mask (land *vs.* water) is overall provided within the SLSTR l1B product. However, some inland waters may be missed and contaminate then the creation of the AOD super-pixel over land. Therefore, an additional test is performed.

For each individual L1B pixel at fine resolution (500 m) labelled as "land" by the L1B surface mask, if

$$NDVI < -0.02$$

then the fine L1B pixel is rejected. Note that the NDVI is directly computed from the SLSTR TOA reflectance.

7.1.5 Numerical Optimization: inclusion of 1st guess for the land surface fit

The joint-aerosol-surface retrieval scheme from the original SU algorithm applies overall low constraints on the surface reflectance in the short wavelengths: *i.e.* no 1st guess is provided on the surface reflectance. The resulted fit within the optimization scheme is fully trusted. In case of high error in the employed land surface model or too low information content, internal experiences have shown that this joint retrieval scheme may become highly instable (*i.e.* a high fraction of AOD values may not be produced), and/or the AOD error may be excessively high. This mostly occurs in case of complex dual-view geometry sampled by the sensor, and/or surface covers associated with a (BRDF) that has a strong spectral signature across the SLSTR channels.

In order to stabilize this optimization scheme and to minimise the AOD error, the idea is to introduce the 1st guess surface reflectance estimated in Sect. 7.1.2 such that it helps to compensate errors introduced by inaccurate assumptions of the original angular land surface model within the joint aerosol-surface retrieval optimization. From analyses reported in Sect. 24, it is deduced that the main error is primarily caused by the significant variability between the geometry and spectral structures, *i.e.*: in case of unfavourable geometry (see Sect. 5.2), the relative aerosol signal is lower & the land surface colour may vary across the view, potentially reflecting a significant spectral signature of the land BRDF. Land covers associated with medium to high vegetation density, sampled by SLSTR in unfavourable geometry, are expected to be the most difficult cases (Aerosol patterns over land covers associated with a high vegetation density are well captured (see Figure 31 & Figure 32). High vegetation covers can reflect up to 20% of spectral variability in the red and green bands, in case of strong backward geometry. This 20% number is the assumed error today associated within the dual-angular land model. This means that the certainty associated with the surface resulting from the joint aerosol-surface fit may be reduced from 100% up to 80% in corresponding cases; the 20% uncertainty being compensated by the 1st guess.

In practice, the following has been assumed & implemented: since the error on the fit land surface reflectance is the key driver of the overall AOD(550 nm) retrieval, it is important its value does represent as much as possible the actual error due to an incorrect AOD retrieval from the SLSTR measurements, and not due to incorrect assumptions in the employed land surface model. If, in specific cases, the used model is inaccurate, it is then necessary to correct it. This is done *via* the overall redefinition of the original error metric of E_{mod} (see Sect. A.3) of the fitted land surface reflectance within the optimization scheme fit for joint aerosol-land as follows:

$$E_{Mod} = (1 - W_{Mod\_spectral}) * E_{Mod\_dual\_angular} + W_{Mod\_spectral} E_{Mod\_spectral}$$

With:

- $W_{Mod\_spectral}$, the weight to be associated with the 1st guess land surface reflectance for its inclusion in the land surface error fit.
- $(1 - W_{mod\_spectral})$, the weight to be considered with the dual-angular land surface model.
- The estimated error $E_{Mod_dual_angular}$on the retrieved land surface reflectance across both views exclusively based on the dual angular land model:

$$E_{Mod\_dual\_angular} = \sum_{\Omega=1}^{2} \quad \sum_{\lambda=1}^{5} W_{Mod\_dual\_angular}(\lambda, \Omega)\left[R_{Meas\_surf} - R_{Mod\_dual\_angular\_surf}\right]\text{^}2$$

$W_{Mod\_spectral}$ is defined such that the 1st guess land surface reflectance, derived from the AFRI red-SWIR LSR model helps to compensate errors introduced by the dual-angular model alone. Such errors mostly occur in 1) unfavourable dual-view geometry (*i.e.* too high dominance of the backward scattering angle), and 2) over land covers with high geometry asymmetry in its BRDF and with an associated significant spectral signature across the dual-views.

The maximal value of $W_{Mod\_spectral}$ is 20%. It is reached if:

- The minimum scattering angle between both nadir & oblique views $\theta_{\min\_dual}$ is no less than the maximum threshold $\theta_{\max\_threshold}$ = 110 deg (see Sect. 5.2).
- **AND** if the measurements are acquired over very highly developed vegetation cover, *i.e.* the AFRI in nadir view is no less than $AFRI_{\max\_nadir\_threshold}$ = 0.95.

The minimal value of $W_{Mod\_spectral}$ is 0%. It is reached if:

- The minimum scattering angle between both nadir & oblique views $\theta_{\min\_dual}$ is no more than the minimum threshold $\theta_{\min\_threshold}$ 100 deg
- **OR** if the measurements are acquired over bare soils with nearly Lambertian geometry properties, *i.e.* the AFRI in nadir view is no more than $AFRI_{\min\_nadir\_threshold}$ = 0.55.

For all cases in between, $W_{Mod\_spectral}$ is built from a linear combination of the thresholds above:

$$W_{Mod_{spectral}} = \max(W_{Mod_{spectral}}) * \frac{\theta_{\min_{dual}} - \theta_{\min\_threshold}}{\theta_{\max_{threshold}} - \theta_{min\_threshold}} * \frac{\text{AFRI} - AFRI_{\min\_nadir\_threshold}}{AFRI_{\max\_nadir\_threshold} - AFRI_{\min\_nadir\_threshold}}$$

The goal of this linear combination is to avoid too sharp transition from an exclusive use (*i.e.* 100%) of the dual-angular land surface model, to its minimum (*i.e.* 80%). Hence within a scene with geometry variability across-scan (from West to East), along-track (from South to North) or over heterogeneous surfaces (from high vegetation to hybrid / urban soils with reduced vegetation), little to medium discontinuities in the retrieved AOD patterns should be observed.

7.1.6 Optimization of spectral channel weighting

In addition to the introduction of the spectral land surface reflectance 1st guess in the optimizations scheme (see Sect. 7.1.5), weights are applied on SLSTR channels over land surfaces. By defaults a weight of 1 (*i.e.* fully reliable) is applied per channel, except for the following conditions:

- Over bright bare soils, a weight of 0.5 (*i.e.* fully 50%) on S2 and S3. The reason is to rely more on S1 in which the land surface reflectance is darker.

- Over vegetation covers:
  - In case of favourable dual-view geometry (see Sect. 5.2), a weight of 0.5 on S1 & S5 due to non-negligible variability & uncertainties associated with vegetation spectral signature.
  - In case of unfavourable dual-view geometry (see Sect. 5.2), a weight of 0 on S1 and S3, and 0.5 on S2. The key rationale is to ensure the right balance between the land surface error metric from the dual-angular & the spectral models in the red band, and to minimize the complex spectral features caused by vegetation canopy in both S1 and S3 channels.

It is acknowledged that such numbers are, at this stage, empirical, and may need further tuning after experiences with a sufficiently large time series.

7.1.7 Numerical Optimisation: Log fit

The particle size distribution is known to show much smoother variability in logarithmic rather than linear scale (Dubovik *et al.*, 2000). Furthermore, using a logarithmic scale should avoid negative AOD retrievals and potentially provide smoother values over cases with low aerosol load. Consequently, the retrieved state vector is modified such that the log(AOD(550 nm)) is fitted. Similar approach is employed in the Bayesian Aerosol Retrieval (BAR) algorithm from MODIS over land (Lipponen *et al.*, 2018).

7.1.8 Adjustment of the AOD pixel resolution

The resolution of the super pixel, or more precisely the actual L2 aerosol pixel, has been modified from 4.5 x 4.5 km^2 to 9.5 x 9.5 km^2, leading to a maximum number of 19 x 19 L1b pixels being considered per L2 aerosol retrieval. The reasons are multiple and cover both scientific & operational aspects to ensure the high timeliness requirement is met:

- The surface reflectance can be very heterogeneous at high resolution while generally aerosol plumes are much smoother. This may lead to complexities in the aerosol-surface decoupling leading to a system noise. The impact of such a noise has been expected, for the first OSSAR-CS3 release, to be not yet properly handled. Hence, it has been preferred to enhance the surface smoothness, especially over land, by increasing the potential number of L1B pixels to average.
- Nadir & oblique views are not necessarily very well co-registered at very high resolution. Also, parallax effects may be encountered over some cases. A small increase in the AOD resolutions allows to minimize the potential errors in dual-view image registration.
- The reduced resolution allows a more efficient computing time w.r.t. the constraints induced by the iterative optimization scheme & operational constraints.
- A resolution of 9.5 x 9.5 km^2 allows to meet the operational user needs regarding the horizontal (and timeliness) requirements, and is compatible with the typical spatial scale of aerosol variability.

In the first tests achieved during the operational deployment of the OSSAR-CS3 v2.0 processor – PB 1.0, a small spatial noise reduction in the was observed in the daily AOD(550 nm) maps. It should be expected that in the future, upon established and stable algorithm maturity level acknowledged by the aerosol community, the spatial resolution could be adjusted again to a

finer resolution. However, the optimal scale will request to be estimated and evaluated on reference cases.

7.1.9 Enhanced *a posteriori* scientific quality filtering

A posterior quality filtering is an important step for identifying AOD pixels associated with poor quality or retrieval problems, and filtering them out in the best parameters (see Sect. 4.2) to be used by most of users. Apart of some instrument anomalies, potential retrieval issues may be caused by: missed clouds in the prior detection, surface contamination by unexpected features such as high ocean colour components. However, a difficulty in filtering is to avoid over-screening of AOD pixels with good quality.

Therefore, the following filtering quality is implemented:

- The original *a posteriori* screening based on the AOD spatial variability (see Sect. A.4) is maintained, but:
    - the threshold on the AOD standard variation is established at a high value of 0.2 to allow screening of obvious cloud residuals (creating a high but artificial AOD spatial variability), but to minimize over-screening of good AOD pixels.
    - In case the 1st criterion is not met and AOD(550 nm) is larger than 0.1: the AOD pixel is screened if the standard deviation is larger than 80% of the average AOD(550 nm) within the 3x3 box.

- Two additional quality filtering specified:
    - The residual of the spectral fit, after the optimization scheme, is analysed *via* the traditional "Khi Square" methodology. If its value is too large w.r.t to *a priori* uncertainties (specific depending on the surface type), the AOD pixel si not conserved. Such AOD pixels are expected to be associated with atmospheric or surface obstruction that can't be correctly represented by the considered aerosol & surface models.
    - In case of unfavourable dual-view geometry (see Sect. 5.2), bright desert soils (such as Sahara) are expected to be highly challenging. At this stage, there are not enough analyses supporting a high reliability of AOD pixels over such areas. Therefore, a radiometric brightness tests is performed based on the S6 SWIR channel. If the associated reflectance is larger than 0.25 in the nadir view, and the dual-view is in unfavourable geometry, the AOD pixel is filtered out. This leads to large gaps over Sahara on a daily basis.

Note that all the scientific *a posteriori* filtering screens the AOD pixels in the best AOD parameters (AOD_550 for ocean, AOD_550_Land for lands). But, all these pixels are still present in the product via the raw AOD parameters (AOD_550_ocea_nonFiltered & AOD_550_Land_NonFiltered).

The enhanced *a posteriori* filtering leads to the following benefits:

- Over oceanic areas, most of snow & melted ice, as well as polar & other types of cloud residuals, originally undetected in the L1B product, are successfully screened (See Figure 28).
- Most of AOD outliers in coastal areas, caused by the presence of high sediment load are filtered out (see Figure 29).

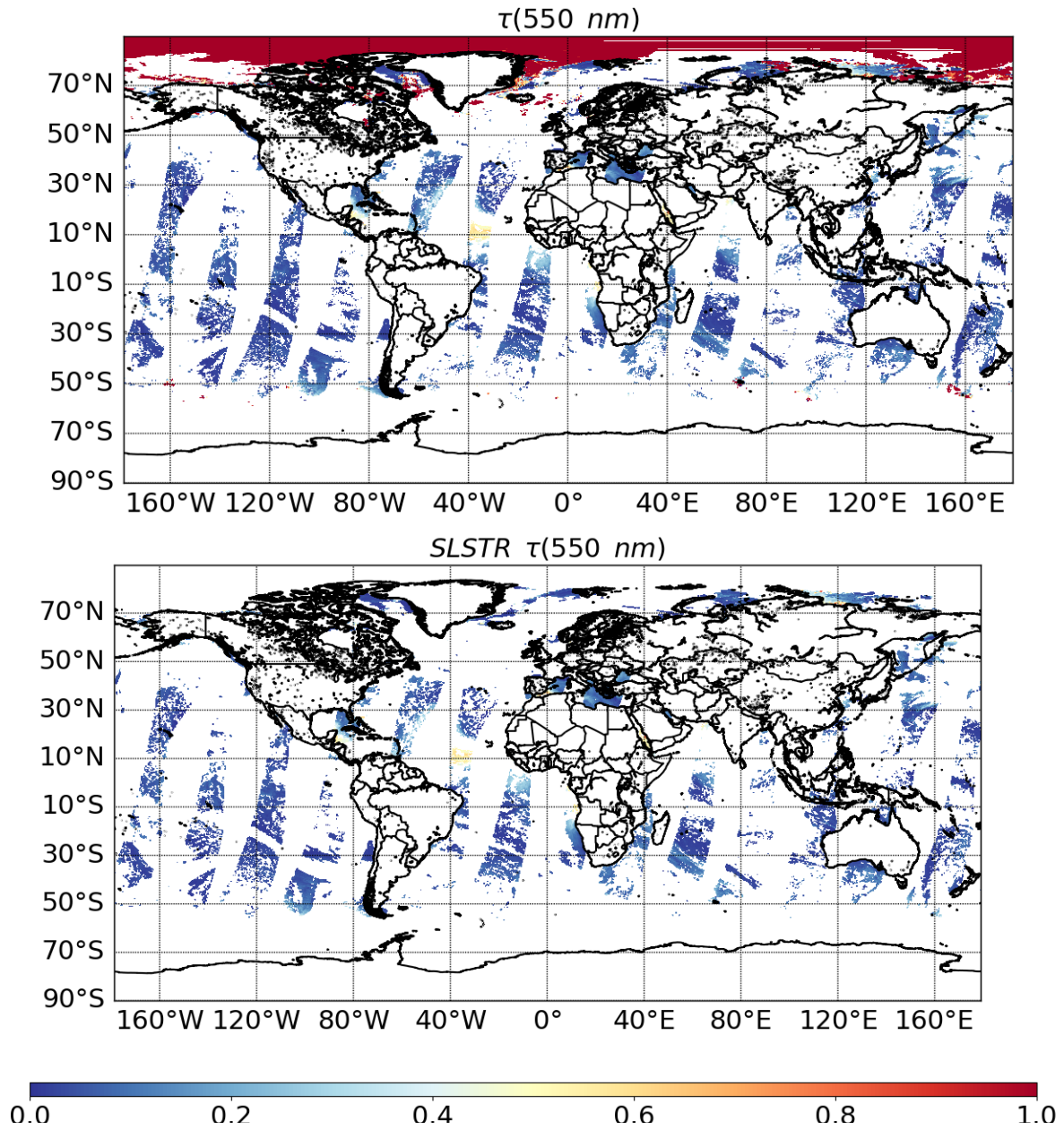

Figure 28: Benefits of *a posteriori* quality filtering on ocean clouds (polar stratospheric), melted snow/ice &other residuals. Case study 30.06.2020 S3A SLSTR. Top = From precursor IPF v1.0 (exclusively based on SLSTR l1B cloud mask). Bottom = from PB 1.0 IPF v2.0.

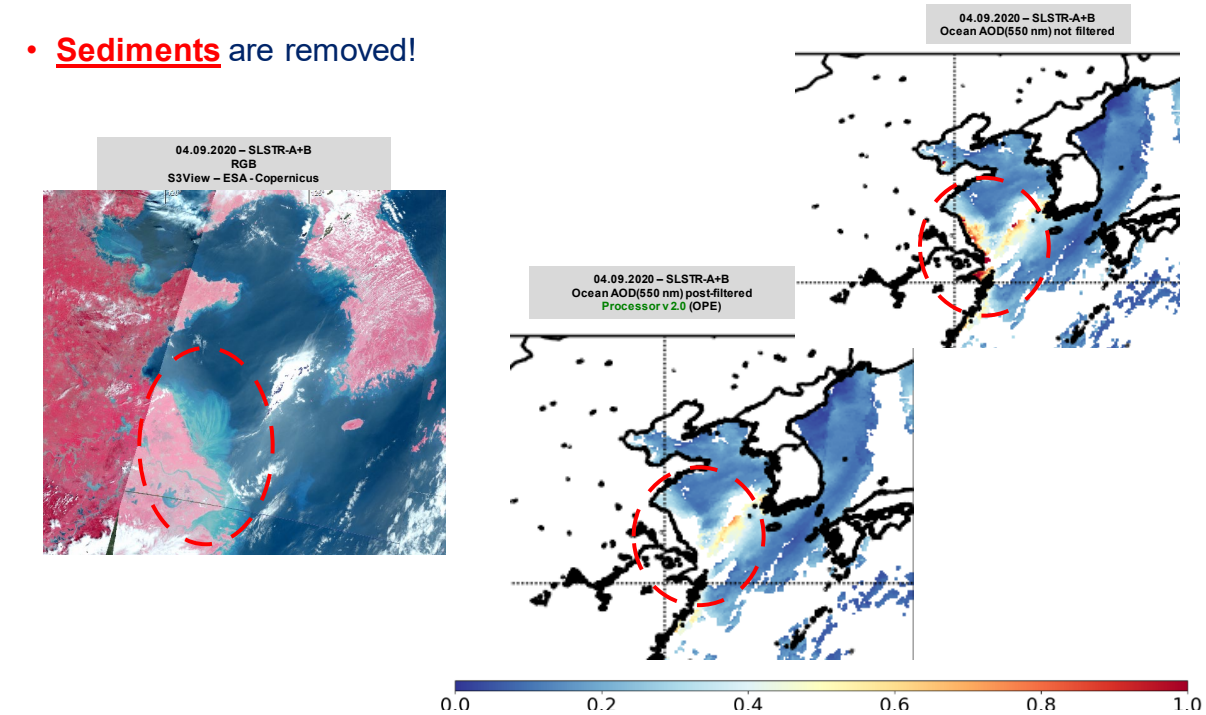

Figure 29: Benefits of *a posteriori* quality filtering over high sediment load in coastal areas. Left: SLSTR RGB; Middle: AOD(550 nm) from IPF v2.0; Right: AOD(550 nm) from IPF v1.0

7.2 Visual illustration of benefits resulting from all combined EUMETSAT evolutions

The combined modifications above have allowed a series of major improvements from the v1 precursor processor baseline:

- Over ocean surfaces:
  - Large positive bias over both background & high dust load are strongly reduced (see Sect. 7.1.1 & Figure 30).
  - High AOD outliers are better filtered out (See Sect. 7.1.9), leading improved land/sea transition and regional statistics.

- Over land surfaces:
  - The overall aerosol signal & associated spatial patterns are better captured & more consistent with the SLSTR Red-Green-Blue (RGB) observations (see Figure 30). There is also less ambiguity with mixture of cloud layers (see Sect. 7.1.3).
  - Aerosol patterns over land covers associated with a high vegetation density are well captured (see Figure 31 & Figure 32), and more consistent with MODIS or VIIRS.
  - AOD retrieval is not only more accurate (lower bias) but also more stable thanks to an improved aerosol-surface decoupling. Consequently, correlations with other operational satellite AOD products show a net increase (see Figure *33*).
  - The quality of the scientific *a posteriori* filtering is improved with a much lower over-screening (see Figure 34). This is also thanks to the most stable optimization scheme leading to smoother AOD patterns.

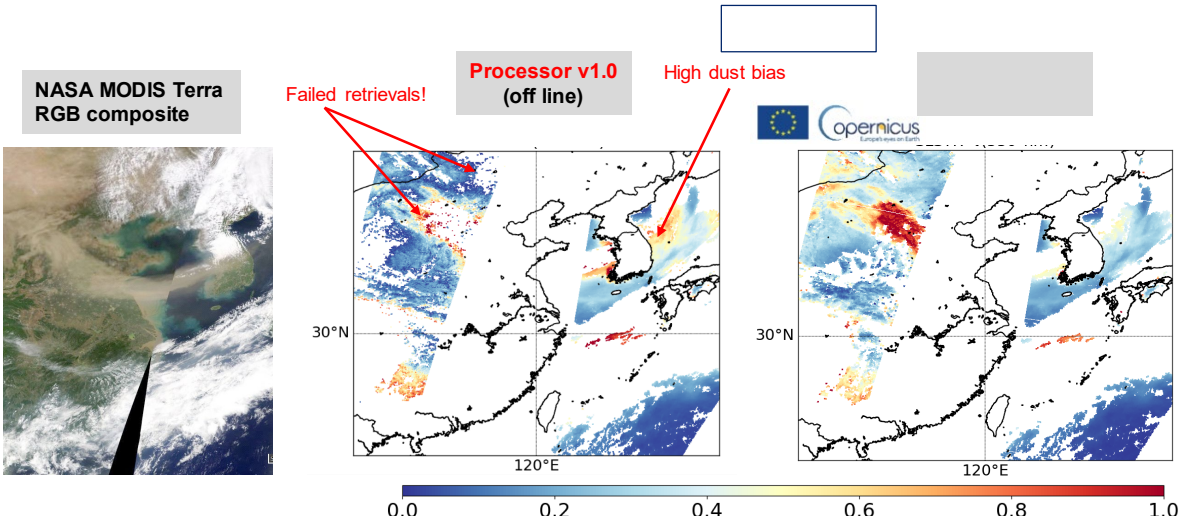

Figure 30: Visual illustration of improvements from IPF v1.0 baseline to IPF v2.0 for a thick aerosol dust plume over land & sea surfaces.

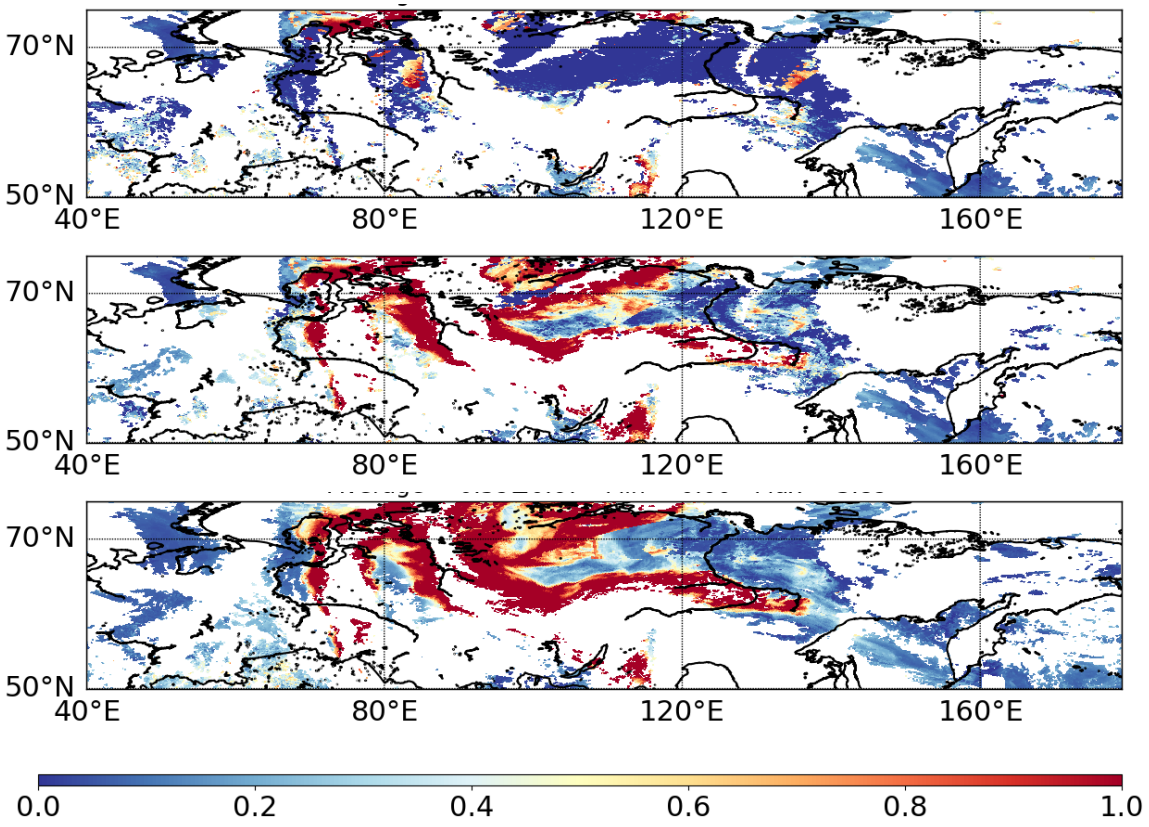

Figure 31: AOD(550 nm) from Siberian smoke aerosol plume due to wildfires on 05.08.2021. Top: precursor IPF v1.0; Middle: OSSAR-CS3 PB 2.0; Bottom: NASA Aerosol DB Collection 1 from VIIRS/SNPP.

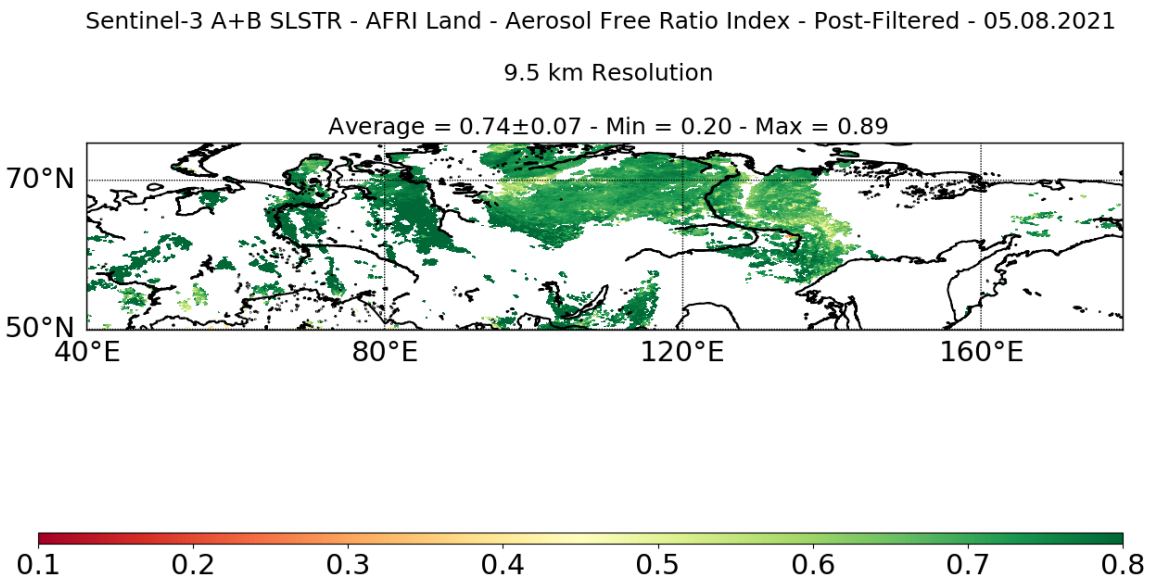

Figure 32: AFRI from OSSAR-CS3 PB 2.0 associated with Siberia wildfires case of **Figure 31.**

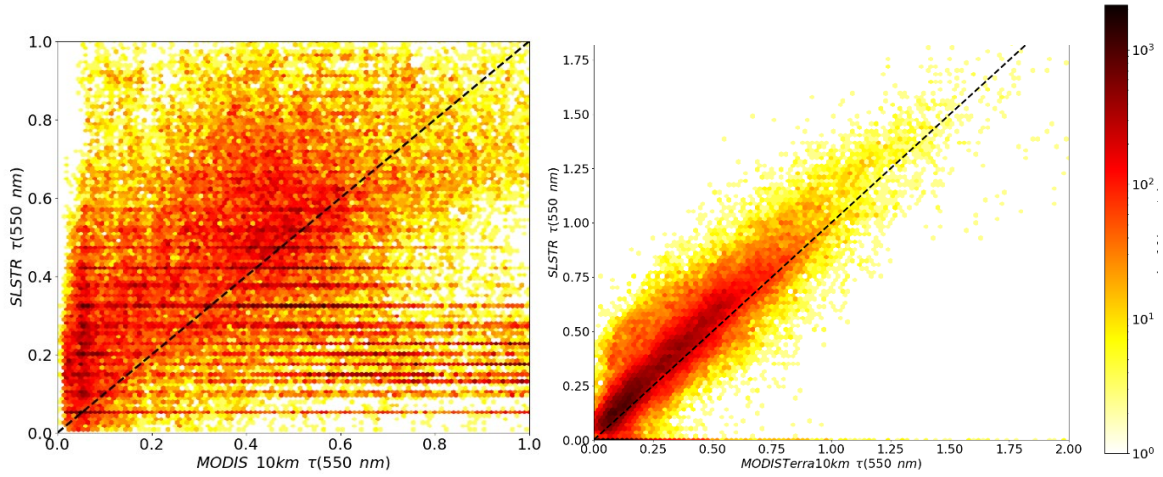

Figure 33: Example of L2 AOD match-up between NASA MODIS Terra Collection 6.1(merged DT/DB algorithm) *vs.* SLSTR S3A NRT AOD over land surfaces exclusively, in East Asia. Left: 3 months from precursor IPF v1.0 (not deployed by EUMETSAT); Right: 1.5 year from IPF v3.0 – Collection 2 (see for more details [RD-4]).

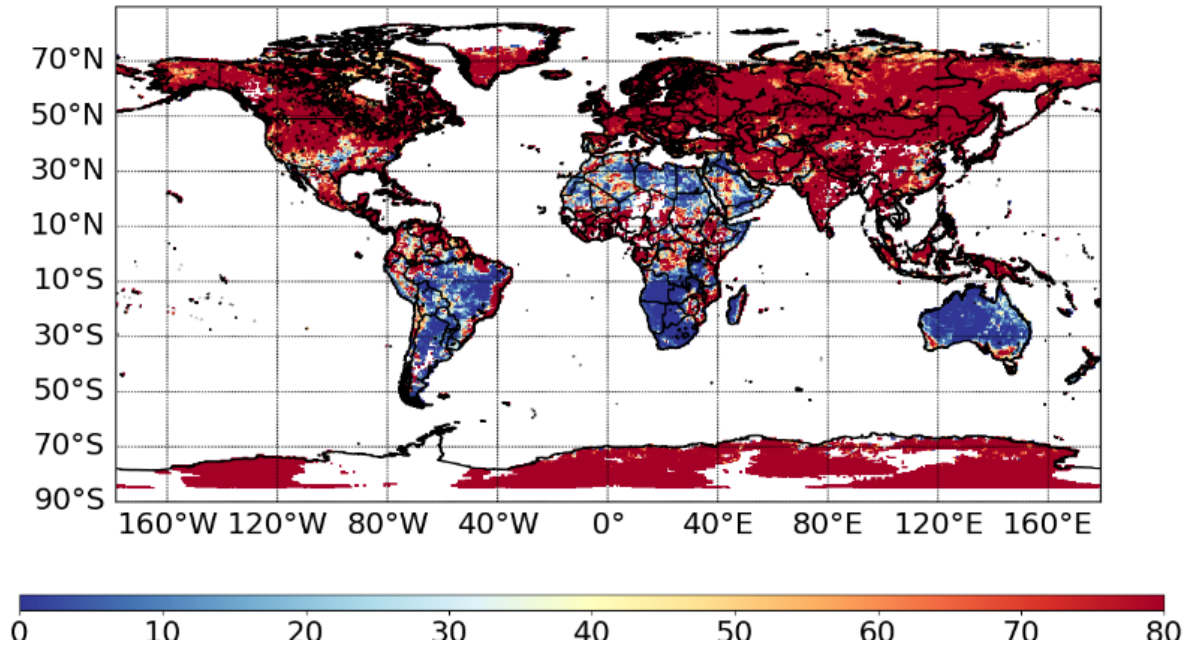

Figure 34: Percentage of AOD pixels non-originally produced over land from IPF v1.0, mostly due to an over *a posteriori* screening.

8 KNOWN LIMITATIONS & OUTLOOK FOR NEXT EVOLUTIONS

The following limitations are known today about the OSSAR-CS3 (see [RD-4} for further details):

- A high cloud-filtering quality is crucial for a reliable operational L2 aerosol product. After all in-depth analysis, EUMETSAT has concluded that the basic cloud mask included in the SLSTR L1B product is not suitable for operational aerosol needs. Therefore, developments are in progress for a global cloud mask module, fully integrated within the OSSAR-CS3 processor. Today, the optical cloud mask over land surfaces is applied directly in OSSAR-CS3. However, the following elements are still coming from that L1B basic cloud mask: 1) thermal infrared tests over land, 2) ocean cloud mask. They are however expected to be completely deactivated and replaced by adequate cloud tests within OSSAR-CS3 during the release of the future Collection 3, as soon as possible within 2022.

- The overall land algorithm baseline has very much evolved. Nevertheless, efforts continue for major evolutions in the next few years. This notably includes i) reduction of the Root Mean Square Error (RMSE) in case of unfavourable dual-view geometry (see [RD-4]), ii) investigation of feasibility to apply multi-temporal constraints as applied in the EUMETSAT OLCI/GRASP concept (see [RD-5]), iii) potential reliable *a priori* land surface reflectance database & improved 1st guess estimations, iv) consolidation of the optimization scheme & associated cost function, etc…

- As further explained in [RD-4], AOD(550 nm) over ocean is overall very good, but the following limitations are known:

    - A low negative bias (of the order -0.015:-0.02) is estimated based on AERONET islands. This estimated bias is mostly observed over ocean background. The exact root cause is currently under investigation in the frame of the Copernicus ACES study procured by EUMETSAT & entrusted by the EC, led by SU as prime contractor, and with the kind review participation from Samuel Remy (HYGEOS, SLSTR QWG member) and Sebastien Garrigues (ECMWF, CAMS). Potential assumptions under confirmation are: i) geometry effects linked to the use of the oblique view, ii) wind correction, iii) white and ocean colour features.

    - Due to the limitations of the SLSTR L1B basic cloud mask, a very high number of SLSTR L1B fine pixels, associated with bright radiances but not necessarily related to clouds, is screened over ocean surfaces. The main assumption is that cloud screening criteria are too stringent and not adequate for aerosol purposes. This leads to i) an under-representativeness of the SLSTR AOD observations in open oceans, and ii) a lower Level 3 (L3) AOD values when averaged over large scales, compared to similar statistic from other space-borne sensors (VIIRS, MODIS). The main reason being that the prior basic cloud mask mostly leaves ocean pixels with dark / low radiances over ocean background (i.e. free of aerosols). Preliminary works based on a prototype ocean cloud mask, internal

at EUMETSAT, start showing encouraging results with an increased L3 SLSTR AOD statistics.

- Quality of SLSTR L1B calibration is of high importance. Currently applied multiplicative coefficients (see Sect. 7.1.1) within OSSAR-CS3 allows a first order of correction. However, secondary calibration issues may remain and are further investigation by EUMETSAT & various external L1 teams. This notably includes: i) non-linearity effects at low radiances, ii) effects of surfaces (dark vs. bright), iii) non-linearity between SLSTR S3A & S3B sensors, etc…

- The following remains to be further investigated, consolidated & validated: i) AOD uncertainty estimation, ii) ancillary output aerosol parameters: Fine Mode Fraction (FMF), ii) dust AOD, iii) Angstrom, iv) Single Scattering Albedo (SSA).

The evolutions of the OSSAR-CS3 algorithm & processor baseline continue, under the sole procurement led by EUMETSAT and associated partners, supported by the EC, in consultation with the operational Copernicus services, SLSTR QWG, and EUMETSAT scientific & technical member state delegates. Investigations for the new IPF v4.0 – PB 3.0 - BC 3 have started with the goal of a potential release in the frame of 2022-2023.

9 ACKNOWLEDGEMENTS

EUMETSAT is very grateful and acknowledges the significant & key contributions from its diverse partners leading to the Optimized Copernicus Sentinel-3 NRT Aerosols processor:

- Swansea university (SU), and the team led by Prof. Dr. Peter North.
- Finnish Meteorological Institute (FMI) & the work achieved in the frame of the EUMETSAT SARP project [RD-2] [RD-3]. The SLSTR Aerosol Retrieval Performance (SARP) project, funded and procured by EUMETSAT, has allowed to investigate the aerosol information content and the capability to retrieve AOD from the SLSTR sensor. Based on state-of-the-art radiative transfer simulations, reference land surface Bidirectional Reflectance Directional Function (BRDF) from the ESA ADAM database, and an independent algorithm (the SLSTR Dual View – SDV), actual aerosol uncertainties as a function of geometry have been characterised for any dual-view radiometers (SLSTR, AATSR).
- The past aerosol developments & validation activities applied to dual-view radiometers supported by the ESA aerosol CCI team and involved experts.
- Feedbacks & supports from CAMS/ECMWF (works from S. Garrigues, M. Ades, R. Ribas), SLSTR QWG (especially S. Remy from Hygeos).
- Cross-fertilisation between Sentinel-3 and PMAP Metop AOD developments by EUMETSAT.
- All EUMETSAT Cloud & Aerosol (CLA), and L2 Marine, and L1 experts & colleagues.
- Results from the internship of Corso Quilici, BSc student, *Evaluation of Sentinel-3 SLSTR AOD in complex environments – Focus on water surfaces*, supervised by the EUMETSAT RSP division.
- Lessons learned from the Sentinel-3 OLCI AOD retrieval feasibility study, based on the multi-pixel approach from the Generalised Retrieval of Aerosol and Surface Properties (GRASP) algorithm.

The following persons are greatly acknowledged for their extensive efforts in reviewing this document and contributions to its enhanced quality:

- Soheila Jafariserajehlou: EUMETSAT remote sensing scientist – Aerosol expert – Synergy NRT PMAP from Metop.
- Loredana Spezzi: EUMETSAT remote sensing scientist – MetImage cloud & related products expert.
- Bertrand Fougnie: EUMETSAT Competence Area Manager for Clouds & Aerosols.
- Bojan Bojkov: EUMETSAT head of Remote Sensing and Products.

10 REFERENCES

Ackerman S., Frey R.A., Baum B.A., Schaaf C., *Discriminating clear-sky from cloud with MODIS – ATBD MOD35*, v6.1, January 2006.

Barbieux K, Hautecoeur O, De Bartolomei M, Carranza M, Borde R. *The Sentinel-3 SLSTR Atmospheric Motion Vectors Product at EUMETSAT*. *Remote Sensing*. 2021; 13(9):1702. https://doi.org/10.3390/rs13091702

Cox, C. and Munk, W. (1954) *Measurements of the roughness of the sea surface from photographs of the Sun's glitter*. J. Opt. Soc. Am., 44, 838–850.

Dubovik, O., Smirnov, A., Holben, B. N., King, M. D., Kaufman, Y. J., Eck, T. F., and Slutsker, I. (2000), *Accuracy assessments of aerosol optical properties retrieved from Aerosol Robotic Network (AERONET) Sun and sky radiance measurements*, J. Geophys. Res., 105(D8), 9791–9806, doi:10.1029/2000JD900040.

Dubovik, O., *et al.* (2006), *Application of light scattering by spheroids for accounting for particle non sphericity in remote sensing of desert dust*, J. Geophys. Res.,111, D11208,doi:10.1029/2005JD006619.

Fougnie B. et al., *Aerosol retrieval from Space' — How does Geometry of Acquisition impact our Ability to Characterize Aerosol Properties*, Journal of Quantitative Spectroscopy and Radiative Transfer, JQSRT_2020_490, (2020).

Heidinger A., Straka W.C., *NOAA NESDIS Center for Satellite Applications and Research – ATBD – ABI Cloud Mask*, v3.0, June 2013.

Hsu, N. C., Lee, J., Sayer, A. M., Kim, W., Bettenhausen, C., and Tsay, S.-C. (2019). *VIIRS Deep Blue aerosol products over land: Extending the EOS long-term aerosol data records*. Journal of Geophysical Research: Atmospheres, 124, 4026– 4053. https://doi.org/10.1029/2018JD029688.

Hutchison, K.D., Roskovensky, J.K., Jackson, J.M., Heidinger, A.K., Kopp, T. J., Pavolonis, M.J, and R. Frey, 2005: *Automated Cloud Detection and Typing of Data Collected by the Visible Infrared Imager Radiometer Suite (VIIRS)*, International Journal of Remote Sensing, **20**, 4681 - 4706.

Karnieli, A, Kaufman, YJ, Remer, L, Wald, A (2001). *AFRI - aerosol free vegetation index.* REMOTE SENSING OF ENVIRONMENT, 77(1), 10-21.

Koepke, P. (1984). *Effective Reflectance of Oceanic Whitecaps*, Applied Optics, 23(11), 1816-1824. Koepke, P. (1984). Effective Reflectance of Oceanic Whitecaps, Applied Optics, 23(11),1816-1824.

Levy, R. C., Mattoo, S., Sawyer, V., Shi, Y., Colarco, P. R., Lyapustin, A. I., Wang, Y., and Remer, L. A.: *Exploring systematic offsets between aerosol products from the two MODIS*

sensors, Atmos. Meas. Tech., 11, 4073–4092, https://doi.org/10.5194/amt-11-4073-2018, 2018.

Lipponen, A., Mielonen, T., Pitkänen, M. R. A., Levy, R. C., Sawyer, V. R., Romakkaniemi, S., Kolehmainen, V., and Arola, A.: *Bayesian aerosol retrieval algorithm for MODIS AOD retrieval over land*, Atmos. Meas. Tech., 11, 1529–1547, https://doi.org/10.5194/amt-11-1529-2018, 2018.

Hsu, N. C., Lee, J., Sayer, A. M., Kim, W., Bettenhausen, C., and Tsay, S.-C. (2019). *VIIRS Deep Blue aerosol products over land: Extending the EOS long-term aerosol data records*. Journal of Geophysical Research: Atmospheres, 124, 4026– 4053. https://doi.org/10.1029/2018JD029688.

Lee, J., Hsu, N. C., Sayer, A. M., Bettenhausen, C., & Yang, P. (2017). AERONET-based nonspherical dust optical models and effects on the VIIRS Deep Blue/SOAR over water aerosol product. Journal of Geophysical Research: Atmospheres, 122, 10,384–10,401. https://doi.org/10.1002/2017JD027258.

Monahan, E.C. and O'Muircheartaigh, I. (1980). *Optimal power-law description of oceanic whitecap dependence on wind speed*, Journal of Physical Oceanography, 10(12), 2094–2099, 1980.

North, P.R.J. (1996), *Three-dimensional forest light interaction model using a Monte Carlo method*, IEEE Transactions on Geoscience and Remote Sensing, 34(5), 946-956.
North, P.R.J., Briggs, S.A., Plummer, S.E. and Settle, J.J., (1999). *Retrieval of land surface bidirectional reflectance and aerosol opacity from ATSR-2 multi-angle imagery*, IEEE Transactions on Geoscience and Remote Sensing, 37(1), 526-537.

North, P.R.J. (2002a). *Estimation of fAPAR, LAI and vegetation fractional cover from ATSR-2 imagery*. Remote Sensing of Environment 80:114–121.

North, P. R. J. (2002b). *Estimation of aerosol opacity and land surface bidirectional reflectance from ATSR-2 dual-angle imagery: Operational method and validation*, J. Geophys. Res., 107, doi:10.1029/2000JD000,207.

Veefkind J.Pepijn, de Leeuw Gerrit, Stammes Piet, Koelemeijer Robert B.A, *Regional Distribution of Aerosol over Land, Derived from ATSR-2 and GOME*, Remote Sensing of Environment, Volume 74, Issue 3, 2000, Pages 377-386, ISSN 0034-4257, https://doi.org/10.1016/S0034-4257(00)00106-1, 2000.

Zhao, T. X.-P., Laszlo, I., Dubovik, O., Holben, B. N., Sapper, J., Tanré, D., and Pietras, C. (2003), A study of the effect of non-spherical dust particles on the AVHRR aerosol optical thickness retrievals, Geophys. Res. Lett., 30, 1317, doi:10.1029/2002GL016379, 6.

Zhou, Y., Levy, R. C., Remer, L. A., Mattoo, S., & Espinosa, W. R. (2020). Dust aerosol retrieval over the oceans with the MODIS/VIIRS dark target algorithm: 2. Non-spherical dust model. Earth and Space Science, 7, e2020EA001222. https://doi.org/10.1029/2020EA001222

APPENDIX A KEY ELEMENTS FROM THE SU SLSTR PROTOTYPE V1.0 MAINTAINED IN THE OSSAR-CS3 PROCESSOR

The elements below are extracted from the precursor ATBD originally dedicated to the SU prototype v1.0. Although, the corresponding processor IPF v1.0 was not deployed by EUMETSAT, these elements are overall maintained with no or minimal changes in the current IPF v3.0. The precursor ATBD was written by Prof. Dr. Peter North & Dr. Andreas Heckel, SU, on 14.10.2016.

A.1 Approximated atmospheric radiative transfer

Satellite observations at optical wavelengths consist of solar radiation scattered by both the atmosphere and the surface back in the direction of the sensor. As a first step, super-pixel TOA radiances LTOA are expressed as reflectances RTOA using:

$$R_{TOA} = \frac{\pi L_{TOA}}{F_0 \cos(\theta_s)}$$

Where F0 is exo-atmospheric solar irradiance. For a given sensor waveband, and atmospheric profile, the relationship between surface directional reflectance Rsurf and top of atmosphere reflectance RTOA can be approximated by the equation:

$$R_{TOA}(\theta_v,\theta_s,\phi) = [R_{atm}(\theta_v,\theta_s,\phi) + T(\theta_s)T(\theta_v)\frac{R_{surf}(\theta_v,\theta_s,\phi)}{1-\rho_{atm}R'_{surf}}]$$

where Ratm denotes the atmospheric path scattering term (TOA reflectance for zero surface reflectance), T denotes atmospheric transmission for either sensor to ground or ground to sensor, and ρatm denotes atmospheric bi-hemispherical albedo. The term R′surf denotes ground reflectance for multiple scattered light, and here we use the approximation R′surf = Rsurf . All atmospheric terms in (2) include the absorption and scattering of fixed gases and water vapour. ECMWF fields included in the L1B product are used to provide surface pressure. Over a completely absorbing surface (*e.g.* over deep dark oceans at infrared wavelengths) the measured TOA radiance is due entirely to the atmospheric path radiance. In contrast, over bright land surfaces the surface reflectance term makes a large contribution to the measured TOA radiance.

A.2 Aerosol model Look-Up-Table (LUT)

A set of aerosol models are required to define the optical properties, and are configurable as a

separate LUT file within the Ancillary Data Sets. Pre-compiled LUTs for a set of candidate aerosol models are used to represent a range of aerosol types, based on mixtures of a reduced set of characteristic 'pure' aerosol types. Under Aerosol CCI the four aerosol types chosen to represent these pure aerosol types are two coarse mode aerosol types (sea salt aerosol, desert dust) and two fine mode (weak absorbing, strong absorbing). All assume spherical particles except for desert dust. Properties are listed in Table 3. Optical properties were calculated using Mie code for the spherical

particles, and T-matrix code for desert dust (Dubovik *et al.*, 2006). The properties are fully documented in the ESA Aerosol_cci Aerosol Model Technical Note. These models are used to form 35 mixtures of aerosol types by interpolation of properties (phase function, SSA) according to each 25% fraction within the total aerosol AOD. The Vector 6S code is then used to compute a LUT giving total column atmospheric radiative properties. In operation radiative properties for a continuous distribution of aerosol property variation (coarse/fine ratio, dust fraction etc…) are estimated by tetrahedral interpolation of properties defined at the LUT breakpoints.

Aerosol component	Refr. index, real part (.55µm)	Refr. Index, imag part (.55µm)	reff (µm)	geom. st dev (σ_i)	variance (ln σ_i)	mode. radius (µm)
Dust	1.56	0.0018	1.94	1.822	0.6	0.788
sea salt	1.4	0	1.94	1.822	0.6	0.788
fine mode weak-abs	1.4	0.003	0.140	1.7	0.53	0.07
fine mode strong-abs	1.5	0.040	0.14	1.7	0.53	0.07

Table 3: Optical parameters for four CCI common aerosol models used. Log-normal parameters for two coarse and two fine mode aerosol components and their associated mid-visible refractive indexes.

A.3 The numerical optimization scheme

The retrieval algorithm is illustrated in *Figure 9: Algorithm baseline for simultaneous surface-aerosol properties (τ and FMF) from SLSTR data. The principle baseline is an iterative inversion based on a fit of derived surface reflectance to a parameterised model (land or ocean), Rmod.*Figure 9. To retrieve the aerosol properties from TOA cloud-free radiances we use a coupled numerical inversion scheme that incorporates the lookup tables derived from the radiative transfer model and a constraint based on a simplified model of land or ocean surface scattering. The basis of the inversion is (i) estimation of surface reflectance (RSURF) for all bands and view angles, for an initial estimate of atmospheric profile, and (ii) iterative refinement of the atmospheric profile to minimise an error metric (E_{Mod}) on the retrieved surface reflectance set.

A set of surface reflectances are calculated for a given atmospheric aerosol model and AOD parameterised by value at 550 nm. An error metric is defined on the surface reflectance set based on a weighted fit to either land or ocean models:

$$E_{Mod} = \sum_{\lambda} \sum_{\Omega} W_{(\lambda,\Omega)} [RSurf_{retr} - RSurf_{mod}]$$

With:

- $RSurf_{mod}$, the simulated surface reflectance either by the ocean or land forward model.
- $RSurf_{retr}$, the surface reflectance as derived from the aerosol retrieval (see Sect. **Error! Reference source not found.**).
- λ, the number of used spectral wavelengths
- Ω, the number of used views.
- $W_{(\lambda,\Omega)}$, the *a priori* uncertainties.

For a given atmospheric profile the optimal free parameters of the land surface model that minimize
$RSurf_{mod}$ are found through the Powell multi-dimensional minimisation routine (Press et al., 1992). For ocean retrieval, the algorithm proceeds with the same inversion framework and aerosol model set as for land but the angular model constraint is simply replaced by a simple metric of fit on the a priori ocean reflectance model. The optimal aerosol properties are found by search for the two parameters (AOD and fine mode fraction) which jointly minimise the estimated error E_{Mod}. Following methods developed in Aerosol CCI, the Brent one-dimensional optimisation method is in two nested iterations: the inner loop to find AOD, and outer loop to find fine mode fraction.

Initialisation of Brent and setting brackets:

1) Run Brent minimisation with climatology Fine Mode Fraction (FMF) to determine upper AOD limit. Use the upper bracket (CX) of this Brent run for all subsequent AOD fits
2) Run Brent for fitting fine mode fraction with limits [0, 1] and starting point at climatology fine mode fraction.
3) Subsequently optimise for each fine mode fraction the AOD using [0, (CX)] as brackets and AOD starting point 0.05.

A.4 *A posteriori* processing

The *a posteriori* processing is a subsequent step after AOD retrieval has successfully finished for a larger region. It is a simple image processing considering all neighbours of a retrieved super-pixel, *i.e.* boxes of 9 (3x3) super-pixels. For an individual AOD retrieval to pass successfully this step of filtering the following criteria need to be met:

- at least 3 neighbouring super-pixels with successful retrievals are required.
- the sample corrected standard deviation of the valid super-pixels in the 3x3 box need to be larger than a given threshold.

A.5 A posteriori AOD uncertainty computation.

Over both land and ocean, the retrieval uses non-linear optimisation of an error function. For a correctly normalised value of Khi_2, the estimate of 1 standard deviation. error in AOD(550 nm) is derived from the second derivative (curvature) of the error surface near the optimal value. The curvature term is estimated by parabolic fit of the error function for surrounding values of AOD(550 nm). The curvature term of the error surface gives a measure of the sensitivity of the location of the minimum to error in model fit. For a steeply curved error surface, the retrieved value of AOD(550 nm) is relatively robust to the estimation of model fit, while for a flat error surface small perturbation in model fit error gives rise to a large error in AOD(550 nm). For example, over bright surfaces where surface reflectance approaches the 'critical point', where the TOA radiance is insensitive to variation in AOD(550 nm) we have high uncertainty in the derived AOD(550 nm).

Once the optimal AOD and fine mode fraction are determined successfully the uncertainty needs to be computed as described above. The estimation of AOD uncertainty requires the curvature of the cost function at the optimal AOD. The curvature corresponds to the second partial derivate of the cost function w.r.t to AOD. Since the second derivate is not available analytically it will be approximated assuming a parabolic behaviour of the cost function around the minimum. To fit the parabola three points are required. The first is the minimum, *i.e.* the optimal AOD with the associated cost. Additionally two points need to be computed. Ideally the additional two points should be close to the minimum and bracket the minimum on both sides. However, the choice of
these points needs to consider the following aspe ts:

- The points should be always inside the AOD range of the LUT.
- Due to computational limits, the cost function is not necessarily smooth on small intervals of AOD, especially if the cost function is relatively flat. This requires the choice of points sufficiently apart from the minimum.
- In cases of dark surface the optimal AOD may account for almost all reflectance signal in some channels. In these cases the retrieval is forced to avoid producing negative surface reflectance by a smooth penalty function for higher AOD. This penalty function leads to a
- steep increase of the cost function not related to the actual uncertainty of the AOD. To safely avoid this kind of situation points will be chosen for AOD smaller than the optimal AOD.

In general the cost is computed on {0.7*τopt, 0.85*τopt, τopt } with τopt being the retrieved AOD at minimal cost. One exception is made for τopt < 0.05 when the lowest point is set to

0.002 instead of 0.7*τopt. As the exact performance of the algorithm and thus the estimation of uncertainty will depend on the actual S3 data it may be required to adjust the absolute range of uncertainties by a scaling factor which will only be determined in the validation phase, after processing actual data. It is however of advantage to prepare for the possibility of a constant scaling factor for land and ocean respectively. Furthermore uncertainties over land should ultimately have a lower limit of 0.02+0.05*τopt . Over ocean a minimum value of 0.02 for uncertainty should be used. In case where the curvature of the cost function is not positive, the corresponding quality flag should be raised and 0.02+0.05*τopt is to be used as default value for uncertainty.

APPENDIX B FREQUENTLY ASKED QUESTIONS (FAQ)

10.1 Where can I download the product?

The product can be downloaded by all public users *via* all EUMETSAT Sentinel-3 data accesses, namely:

- The Copernicus Online Data Access (CODA): https://coda.eumetsat.int/#/home
- The EUMETSAT long-term archive data centre: https://www.eumetsat.int/eumetsat-data-centre

10.2 Where can I find all websites & public documentation?

The following public information can be found online *via* the EUMETSAT webPages:

- Operational Sentinel-3 atmospheric portfolio under EUMETSAT responsibility: Atmospheric composition | EUMETSAT
- The operational OSSAR-CS3 processor & associated product: Copernicus Sentinel-3 NRT Aerosol Optical Depth | EUMETSAT

Public visualization of the products is available for every day on the EUMETSAT Monitoring & Evaluation of Thematic Information from Space (METIS): https://metis.eumetsat.int/aod/index.html

10.3 I need help / I have questions. Who shall I contact?

Please contact directly the EUMETSAT help desk office: OPS@eumetsat.int

10.4 What are the differences between PB 1.0 & PB 2.0?

The main differences are:

- The implementation of the optical cloud mask over land surfaces leading to a strong reduction of cloud residuals & AOD outliers (see Sect. 7.1.3).
- The enhanced AOD retrieval quality over land surfaces thanks to the optimized associated algorithm baseline (see Sect. 7.1.2, 7.1.5) leading to a significant bnais reduction.

See the EUMETSAT Product Notice (PN) of OSSAR-CS3 Collection 2 [RD-6] for further details.

10.5 How can I build a consistent time series?

To build a consistent time series:

- Over ocean surfaces: aerosol retrievals are identical between PB 1.0 & 2.0. So, a consistent time series can be built starting from August 2020 available on-line.
- Over land surfaces, it is strongly advised to build a time series with data online by only starting with the PB 2.0 since its public release in October 2021.

To expand the time series above, EUMETSAT regularly leads partial reprocessing campaigns from its off-line environment. To get access to these data, a request shall be sent by contacting the EUMETSAT help desk office: OPS@eumetsat.int.

10.6 How can I remain up-to-date about the coming evolutions or news?

The best is to follow regularly the EUMETSAT news on its webpage https://www.eumetsat.int/.
Another way is to enrol within the Sentinel-3 validation Team (S3VT) atmosphere sub-group co-chaired by EUMETSAT & ESA https://www.s3vt.org/QuickEventWebsitePortal/sentinel-3-validation-team-s3vt/esa/ExtraContent/ContentPage?page=9. The S3Vt Atmosphere meets regularly via dedicated workshops offering then possibility to directly interact with the agency experts.

10.7 I'd like to report or discuss some of my validation results. Where shall I bring them?

As mentioned above, the best is to join the S3VT atmosphere sub-group.

10.8 Are all the SLSTR aerosol products from the different agencies and research teams overall the same?

Each Sentinel-3 aerosol retrieval performed by agencies, institutes, research groups is overall unique. Although some consistencies may be found sometimes, users are advised to consider any existing processors as unique and independent of each other. Users shall also bear in mind their overall significant differences in terms of algorithm baseline & processor capabilities (see Sect. 3.1).